WIRELESS NETWORK CODING FOR MULTIPLE UNICAST TRANSMISSIONS

A THESIS SUBMITTED TO
THE GRADUATE SCHOOL OF NATURAL AND APPLIED SCIENCES
OF
MIDDLE EAST TECHNICAL UNIVERSITY

TUĞCAN AKTAŞ

IN PARTIAL FULFILLMENT OF THE REQUIREMENTS
FOR
THE DEGREE OF DOCTOR OF PHILOSOPHY
IN
ELECTRICAL AND ELECTRONICS ENG.

JANUARY 2014

Approval of the thesis:

WIRELESS NETWORK CODING FOR MULTIPLE UNICAST TRANSMISSIONS

submitted by **TUĞCAN AKTAŞ** in partial fulfillment of the requirements for the degree of **Doctor of Philosophy in Electrical and Electronics Eng.   Department, Middle East Technical University** by,

Prof. Dr. Canan Özgen
Dean, Graduate School of **Natural and Applied Sciences**
————————————

Prof. Dr. Gönül Turhan Sayan
Head of Department, **Electrical and Electronics Eng.**
————————————

Assoc. Prof. Dr. Ali Özgür Yılmaz
Supervisor, **Electrical and Electronics Eng Dept,METU**
————————————

Examining Committee Members:

Prof. Dr.Yalçın Tanık
Electrical and Electronics Engineering Dept., METU
————————————

Assoc. Prof. Dr. Ali Özgür Yılmaz
Electrical and Electronics Engineering Dept., METU
————————————

Prof. Dr. Mete Severcan
Electrical and Electronics Engineering Dept., METU
————————————

Prof. Dr. Elif Uysal Bıyıkoğlu
Electrical and Electronics Engineering Dept., METU
————————————

Assist. Prof. Dr. Ayşe Melda Yüksel Turgut
Electrical and Electronics Engineering Dept., TOBB ETÜ
————————————

Date: 21.01.2014

I hereby declare that all information in this document has been obtained and presented in accordance with academic rules and ethical conduct. I also declare that, as required by these rules and conduct, I have fully cited and referenced all material and results that are not original to this work.

Name, Last Name: TUĞCAN AKTAŞ

Signature   :

ABSTRACT

WIRELESS NETWORK CODING FOR MULTIPLE UNICAST TRANSMISSIONS

Tuğcan Aktaş,

Ph.D., Department of Electrical and Electronics Eng.

Supervisor   : Assoc. Prof. Dr. Ali Özgür Yılmaz

January 2014, 82 pages

In this work, firstly we propose a practical and effective cooperative communication technique based on network coding (NC) in order to mitigate the detrimental consequences of fading in wireless channels. We base our formulation on multiple unicast transmissions which is the natural way of communication in many modern wireless networks. The proposed technique utilizes spatial diversity through cooperation between overhearing nodes which carry out distributed encoding operations dictated by the generator matrices of chosen linear block codes. In order to exemplify the technique, we make use of greedy codes over the binary field and adapt a Time Division Multiple Access (TDMA) type use of the channel. We show that arbitrary diversity orders can be flexibly assigned to the nodes according to the separation vector corresponding to the generator matrix. In addition to the optimal detection rule for deciding on the information symbols transmitted in the network, we present a novel network decoder which relies on the sum-product (SP) algorithm running on a Tanner graph that is constructed for the underlying distributed block code. This network decoder is shown to be both advantageous in terms of its low-complexity and its performance

which is very close to that of the optimal one. We further show asymptotic superiority of NC over a plain Automatic Repeat-reQuest (ARQ) method that utilizes the wireless channel in a repetitive manner without NC and present related rate-diversity trade-off curves.

In the second part, we derive approximate average bit-error-rate (BER) expressions for the proposed network coded system. In order to reach these expressions, we initially consider the cooperative systems' instantaneous BER values that are commonly composed of Q-functions of more than one variable. For evaluating the expectation integrals involving these Q-functions easily, we investigate the convergence characteristics of the *sampling property* for integrand functions and generalize this property to arbitrary functions of multiple variables. Then, we adapt the equivalent channel approach to the network coded scenario for ease of analysis and propose a corresponding suboptimal network decoder based on the Cooperative-Maximal Ratio Combining (C-MRC) method. Finally, by combining the sampling property, equivalent channel assumption and C-MRC technique, we reach closed form average BER expressions. Through simulations, the agreement of the obtained closed form expressions with the performance of the proposed network coded system is demonstrated in a wide SNR range. As one of the initial studies from the communication theory window in the field of NC, the proposed system model and the analysis techniques are expected to serve as the building blocks for the design and the performance analysis of general network coded systems with larger number of nodes and practical considerations like channel coding, resource reuse, channel estimation, multi-user interference management, etc.

Keywords: Wireless network coding, linear block codes, detect-and-forward, unicast transmission, sum-product decoding, fading channels, BER analysis, Q-function.

ÖZ

BİRDEN ÇOK TEKEGÖNDERİM İÇİN KABLOSUZ AĞ KODLAMASI

Tuğcan Aktaş,

Doktora, Elektrik ve Elektronik Mühendisliği Bölümü

Tez Yöneticisi   : Doç. Dr. Ali Özgür Yılmaz

Ocak 2014, 82 sayfa

Bu çalışmanın ilk kısmında, kablosuz kanallarda sönümlemenin bozucu sonuçlarıyla başa çıkmak için ağ kodlamayı temel alan, kolay uygulanabilir ve etkili bir işbirlikli haberleşme tekniğini öneriyoruz. Önerilerimizin kurgusunu günümüzde kullanılan birçok haberleşme sisteminde de doğal olarak karşılaşılan birden fazla tekegönderim senaryosu üzerinde şekillendiriyoruz. Önerilen teknik, birbirini duyan ve doğrusal blok kodların üreteç matrislerini temel alarak dağıtık bir şekilde kodlama görevi yapacak düğümler üzerinden elde edilecek uzamsal çeşitleme kazancından faydalanmaktadır. Tekniğin örneklenmesinde, ikili alanda tanımlanmış greedy blok kodlarını kullanıyoruz ve Zaman Bölümlemeli Çoklu Erişim tarzında kanal kullanımını uyarlıyoruz. Bu kodlar aracılığıyla, seçilen üreteç matrisine ait ayrım vektörünün belirlediği farklı çeşitleme derecelerinin istenilen düğümlere atanabileceğini gösteriyoruz. Ağda iletilen bilgi sembollerinin eniyi tespit kuralıyla belirlenmesi yanında, dağıtık blok koda göre inşa edilmiş bir Tanner çizgesi üzerinde yinelemeli olarak çalışan toplam-çarpım algoritmasına dayanan özgün bir ağ kodu çözücü yapısı sunuyoruz. Bu ağ kod çözücünün hem düşük işlem yükü sağlaması hem de eniyi tespit kuralına ya-

kın başarımı sergilemesi nedeniyle avantajlı olduğunu gösteriyoruz. Buna ilaveten ağ kodlamalı tekniğin, kablosuz kanalı herhangi bir kodlamaya başvurmaksızın ardışık olarak kullanan yalın Otomatik Tekrar İsteği (ARQ) tekniğine olan üstünlüğünü ortaya koyuyoruz ve iki teknik arasındaki başarım farkını ilgili veri oranı - çeşitleme derecesi ödünleşimi eğrileri ile açıklıyoruz.

İkinci kısımda, önerdiğimiz ağ kodlamalı sistem için yaklaşık ortalama bit hata olasılığı ifadelerini türetiyoruz. Bu ifadelere ulaşmak için öncelikle işbirlikli sistemlerin anlık bit hata olasılığı ifadelerinde sıklıkla karşılaşılan ve birden fazla değişkene bağlı Q-fonksiyonlarını ele alıyoruz. Bu Q-fonksiyonlarını içeren beklenti integrallerini kolaylıkla hesaplayabilmek için *örnekleme özelliği* adı verilen bir yöntemin yakınsama karakteristiğini inceleyip bu özelliği birden çok değişkenin herhangi bir fonksiyonu için geçerli olacak şekilde genelleştiriyoruz. Sonrasında analiz basitliğini sağlamak için eş değer kanal yaklaşımını ağ kodlamalı senaryoya uyarlayıp, karşılık gelen eniyi altı ağ kodu çözücüsünü İşbirlikli-Enbüyük Oran Birleştirmesi metodu üzerinden tanımlıyoruz. Son aşamada, örnekleme özelliğini, eşdeğer kanal yaklaşımını ve İşbirlikli-Enbüyük Oran Birleştirmesi metodunu birleştirerek kapalı formdaki bit-hata-olasılığı ifadelerine ulaşıyoruz. Elde edilen bu kapalı form ifadelerin önerilen ağ kodlamalı sistemin başarımı ile geniş bir Sinyal-Gürültü-Güç Oranı aralığı içindeki uyumu benzetimler aracılığıyla gösteriliyor. Ağ kodlaması alanındaki haberleşme penceresinden bakan ilkin çalışmalardan biri olarak, önerdiğimiz sistem modeli ve analiz tekniklerinin; daha çok sayıda düğümden oluşan ve kanal kodlaması, kaynakların yeniden kullanımı, kanal kestirimi, çok kullanıcılı girişim yönetimi ve benzeri pratik konuların değerlendirildiği daha genel ağ kodlamalı sistemlerin tasarım ve başarım analizinde yapıtaşlarını teşkil etmesi beklenmektedir.

Anahtar Kelimeler: Kablosuz Ağ Kodlaması, doğrusal blok kodlar, tespit-et-ilet, tekegönderim, toplam-çarpım kod çözümü, sönülemeli kanallar, bit-hata-olasılığı analizi, Q-fonksiyonu.

To my dearest friend

ACKNOWLEDGMENTS

their help, and I am extremely grateful for having such compassionate parents. My sister, Tuğçe also helped me a lot with her patience and strong support in spite of all my complaints related to my studies and project work. Last but in no way the least, I thank my girlfriend, Pınar, for her love and friendship. Owing to her motivating words, I have easily cleared many of the hurdles both in my academic life and personal life. It has been a great enjoyment for me to work in a research project together with her just like it has always been a pleasure to share the lively discussions about everything in life.

TABLE OF CONTENTS

LIST OF FIGURES

FIGURES

LIST OF ABBREVIATIONS

AF	Amplify-and-Forward
APP	A Posteriori Probability
ARQ	Automatic Repeat-reQuest
AWGN	Additive White Gaussian Noise
BER	Bit-Error-Rate
BPSK	Binary Phase Shift Keying
C-MRC	Cooperative-MRC
CRC	Cyclic Redundancy Check
CSI	Channel State Information
DetF	Detect-and-Forward
DF	Decode-and-Forward
GF	Galois Field
ISI	Inter-Symbol Interference
LDPC	Low-Density-Parity-Check
LLR	Log-likelihood Ratio
MAP	Maximum a Posteriori
MDS	Maximum Distance Separable
ML	Maximum Likelihood
MRC	Maximal-Ratio-Combining
NC	Network Coding
PC	Parity Check
pdf	Probability Density Function
PMF	Probability Mass Function
SNC	Selective Network Coding
SNR	Signal-to-Noise Ratio
SP	Sum-Product
TDMA	Time Division Multiple Access
ZMCSCG	Zero Mean Circularly Symmetric Complex Gaussian

CHAPTER 1

INTRODUCTION

Due to the multipath and shadowing effects in the radio communication medium, one frequently observes random deviations in the amplitude of the received signal. This effect is named as fading and can cause severe degradation in the performance of the wireless communication systems. In order to counteract these effects of fading, many ways of creating diversity for the transmitted data have been proposed. Utilizing the spatial diversity resulting from the broadcast nature of the wireless communication medium, cooperative communication [41] has been of great interest in recent years. Through cooperation between nodes, the overall reliability and the throughput of the system can be improved by mitigating the deteriorating effects of fading. The basic cooperation scenario assumes a dedicated relay node assisting the communication between a source and a destination node [41]. In [11, 30] three methods to be used by relay nodes are described: amplify-forward (AF), decode-forward (DF) and detect-forward (DetF). The AF method attains full diversity, whereas other two cannot, unless the propagation of errors resulting from the decoding/detection operation is avoided, for example by using a selective transmission strategy that advocates the forwarding of only sufficiently reliable packets. One of the various ways to handle this problem is using Cyclic Redundancy Check (CRC) based methods, which results in loss of spectral efficiency due to drop of a packet with only a few bit errors. An on/off weighting based on relay signal-to-noise power ratio (SNR) is given in [38]. Weighting of the signals either at the relay or at the receiver using the relay error probability is proposed in [46,47]. Yet another idea is transmitting the log-likelihood ratios (LLR) of bits [53]. However, the soft information relaying methods in [46,47,53] suffer from quantization errors and high peak to average ratio problems. In addition, the

1

AF method requires hardware modifications on modern-day communications systems and the DF method leads to high complexity decoding operations especially for the relays. As an alternative, relays may use the low-complexity DetF method. This low complexity takes its roots from the fact that a DetF-type relay simply hard-detects the incoming symbols and forwards these detection results to the destination node without any channel decoding operation [30]. If the error probabilities at relays are known and the maximum a posteriori probability (MAP) detection is employed at the receiver, DetF is shown to prevent error propagation in [11]. One may also adhere to the equivalent channel approach in conjunction with the cooperative maximal-ratio combining (C-MRC) method which reaches a decision based on a weighted sum of observations again by utilizing the source-relay channel reliability information [46]. Both of these techniques are shown to achieve full-diversity order with DetF-type relaying.

NC was initially proposed to enhance network throughput in wired systems with error-free links of unit capacity [1]. In [1], authors proved that coding at the intermediate (relay) nodes may improve the information flow rate in the network. Again for wired unit capacity links assumption, the good performance of random linear NC is exhibited [19]. Later many studies investigated the properties and limits of network coding strategies for both wired and wireless operations [13]. In network coded wireless communications, which can be seen as an extension of the basic cooperative communication scenario, the throughput in the whole network is shown to be improved by combining data packets of many sources in a single packet via Galois Field (GF) operations at the intermediate node [28]. In this way, NC is shown to create extra diversity, reduce routing overhead, and introduce MAC layer gains in currently utilized wireless communication systems with small modifications. Although most of the work in the literature concentrate on multicast transmission [13]; we deal with a network involving multiple unicast transmissions, which is inherent in real-life scenarios. Hence we formulate a multiple unicast transmission problem such that each unicast transmission observes a distinct diversity order that is to be improved via spatial opportunities. Moreover, in this study, we aim to devise analysis methods for the BER performance of wireless network coding scenarios with DetF-type intermediate nodes under realistic quasi-static Rayleigh fading channels by starting our analysis

2

from the basic relayed communication model.

Given a intermediate node combining strategy, which we represent by a generator matrix and a vector of transmit schedule, we investigate the diversity order for information bit of each source, which can be unequal in general. We propose a novel method for designing the generator matrix based on linear block codes over the binary field. The proposed method is flexible in that any set of desired diversity levels for the sources can be achieved with the highest NC rate possible. The diversity analysis relies on an optimal MAP decoder at the destination which employs the reliability information of the intermediate nodes and avoids loss of diversity due to error propagation [11, 21]. However, The numerical complexity of the given optimal decoder can be impractical for increasing network size or number of transmissions. Thus we propose a practical approximation: the sum-product (SP) network decoder, which has been shown to perform quite close to the Shannon's capacity limit for decoding the family of low-density parity-check (LDPC) codes [40]. We also derive the modified Tanner graph structure for any NC system by including the reliability information in the observations which result from possibly incorrect network coded data bits and the SP algorithm iterates on this graph.

A study based on flexible network codes in a two-source two-relay system with emphasis on unequal error protection is [22], where authors propose a suboptimal detection rule (distributed minimum distance detector) that is known to result in diversity order loss. Our scheme captures full diversity due to the use of the SP detector with intermediate node reliability information. In [49], a multicast scenario is investigated (again under additive white Gaussian noise (AWGN) assumption) for obtaining an optimal energy allocation scheme in order to minimize bit error rate at the sink nodes. In [50], performance of a multiple hop network without fading is analyzed in terms of effects of the bit errors at the relays utilizing a technique known as error event enumeration. Similarly in [51], optimal detection rule to be used at the destination node is presented for AWGN channels in addition to the description of a genie-aided decoder which yields a lower bound on the performance of the optimal detector. Different than [50] and [51], we consider faded wireless links and give optimal detection rule corresponding to this realistic scenario. Futhermore, the operation at the intermediate nodes in our scheme is DetF as opposed to the more complex DF in [50, 51].

One of the studies closest to ours is [52], where the NC operation is fixed in construction yielding very large Galois field (GF) sizes for increasing network size and relay nodes carry out complicated DF operation for each transmission they overhear. Similarly in [45], DF is used in a fixed single-relay two-user scenario in order to provide diversity-multiplexing trade-off for NC. However, our results indicate that any diversity order can be achieved for any unicast transmission even with the GF of size 2 by using linear block codes as the network codes and simple DetF. Also independently from our work, in [20, 21], results concerning diversity analysis for a system model resembling ours have been obtained. Similarly in a recent work [14], additional coding gain analysis is given for a multi-source multi-relay network with relays having no data to be transmitted. Our model is more general in the sense that each node acts both as a source node with its own data to be conveyed over the network and as an intermediate node serving as a means for combining and relaying others' data. Moreover, the proposed detection rules of [14, 20, 21] result in exponential decoding complexity in the number of transmissions, since they are based on maximum likelihood sequence estimation. Recently in [32], a wireless broadcast network with block erasures is considered and a network coding scheme is proposed for retransmissions. The improvement in the number of retransmissions for the downlink channel with respect to the conventional automatic-repeat-request mechanism is clearly shown. Another recent work [44] identifies the diversity-multiplexing trade-off for a NC system, in which multiple access to the channel is allowed to be non-orthogonal. On the other hand, our model with orthogonal access of the nodes to the channel does not require a complex successive interference cancellation technique to be implemented at the destination node. We should further note that we assume that the nodes access the channel using the simple Time Division Multiple Access (TDMA) method over orthogonal time slots. Based on our model, it is shown in [23] that further improvements on diversity-multiplexing trade-off are possible with GF(q) operation. In addition, our scheme is also proved to be practical especially for the systems with no channel state information at the transmitting nodes (no CSIT). One final note may be on the applicability of our proposed system model to the wireless communication systems that are currently in use. From that point of view, although we propose simple encoding and decoding methods with practical implementation issues in mind, one still has to put effort on the following topics for including the ideas detailed in this work

within a more realistic communication system. First of all, in real world, almost all similar systems operate with the additional protection of the channel codes. Hence one also should spend time on joint design of both the encoders and more importantly the decoders that consider the channel and the network codes simultaneously. Especially, in the scenarios that are affected by mobility of the nodes, the temporal diversity within the duration of a packet may be obtained through a careful selection of channel codes and interleaver structures. Secondly, the results obtained in this work should also be investigated for systems that incorporate larger Galois field sizes for NC and larger constellations for modulating the coded data with increased spectral efficiency. Moreover, we should also take the possibility of broken links between users in a network, because in reality not every node is successfully heard by every other node in a given network. Hence the fully-connected network assumption in this work should be relaxed and adaptive network codes based on the instantaneous topology of the network should be constructed. Finally, in a much larger network than the ones considered in this work, hierarchical structures for NC operations and also re-use of temporal resources (since now distant nodes will not create interference to each other by simultaneous transmissions) must be adapted for improving performance. In this sense, the results presented in this work may serve as the directions for the design of a NC sub-network with several nodes that are quite close to each other.

Regarding performance of the equivalent channel approximation together with the C-MRC method at the destination side, the diversity order analysis for the basic relayed communication scenario under Rayleigh fading is made in [46] and [29], where the authors reach the result that the related system achieves a diversity order of 2. This result is obtained by applying a number of approximations on the end-to-end instantaneous and thus average BER expressions and the final average BER expressions are very loose in general. Recently in [36], authors use C-MRC for the analysis of single-relay network coded communication. Here, in this work, one of our goals is deriving a closed-form approximate average BER expression for the basic relayed communication scenario, which is tight in the mid-to-high SNR region and that gives us the coding gain term in addition to the previously established diversity order. In obtaining this closed-form expression, we make use of the sampling property of the Q-function introduced in [24, 25], where the expectation integrals required for inves-

tigating the average BER performance of cooperative systems are handled through an approximation on the Q-function appearing in the instantaneous BER functions. We generalize the sampling property to more general arguments of the Q-function with possibly more than one variables [4]. Such a general form of sampling property is avoided in [24, 25] by expressing any function of more than one variables as sum of single-variable functions through approximations which yield coding gain offsets in the final expression. Moreover, we try to characterize the low-SNR region approximation problem with the sampling property, which is also pointed in [26]. Different than [26], we analyze the *convergence rates* for the constituent functions of the integrand function in order to distinguish a threshold value above which the Q-function related part can safely be approximated by a Dirac-delta generalized function. Finally, we adopt the equivalent channel approach and the C-MRC technique to the network coded scenario with multiple intermediate nodes introduced in [3, 6] and analyze the average BER for a sample network again by using the generalized sampling property for the Q-function that we propose. Both for the basic cooperative system and the sample network coded cooperative system, we compare the closed-form expressions we derived with the simulated BER curves and observe a very good agreement between them [5]. As one of the initial studies from the communication theory window in the field of NC, the proposed system model and the analysis techniques are expected to serve as the building blocks for the design and the performance analysis of general network coded systems.

The major goal in introducing *practical NC/decoding methods* is to improve the diversity order of a network through cooperation with the overall rate of transmission in mind. The contributions of our work can be listed as follows.

- A generalized wireless NC scenario with nodes possessing both relay and source roles and its diversity analysis.

- Design of novel network codes based on close-to-optimal linear block codes.

- Investigation of greedy codes and maximum code rates for desired diversity levels.

- Application of the SP algorithm for decoding network codes with relay reliability information.

- Generalization and a detailed inspection of the Q-function's sampling property for approximating the expectation integrals observed in cooperative communication systems.

- Extension of the equivalent channel model and the C-MRC method from the basic cooperative scenario to the NC scenario so that the resulting expectation integrals are covered by the generalized sampling property.

- Derivation of the approximate closed-form average BER expressions for characterizing the performance of a given NC scenario.

The rest of this work is organized as follows. In Chapter 2, we introduce the system and the signal models for the proposed NC system in addition to the basic cooperative scenario, which will form the basis especially in the analysis of NC system. Afterwards, we continue with the identification of the design criteria for constructing the linear block codes that directly determine the distributed NC rules in the proposed system in Chapter 3. We also present some asymptotic results based on the rate-diversity order trade-off curves for the proposed NC method and make comparisons to a network operating without NC. In addition to the MAP-based optimal and suboptimal detection rules given in Chapter 2, we propose a novel SP network decoder with linear complexity order in Chapter 3 and this section includes the numerical results for the mentioned network encoding/decoding methods. In the second part, starting with Chapter 4, we concentrate on the analysis of the end-to-BER performance of the proposed NC scenario. Chapter 4 also demonstrates the agreement of these obtained analytical expressions with the simulation results for a sample NC scenario. Finally, Chapter 5 draws conclusions and poses some possible paths for future work.

CHAPTER 2

PROPOSED DETECT-AND-FORWARD TYPE NETWORK CODED COOPERATIVE COMMUNICATION SYSTEM MODEL AND OPTIMAL DETECTION RULES

This section starts with a brief description of the basic cooperative scenario of a system including a single relay node that assists the communication between a source and a relay node. Afterwards, we give the details of the network coded cooperative communication system with more than one source node each of which is acting as an intermediate node to other node(s). Here the intermediate node has the functionality of combining other nodes' and its own data packets through network coding operations in addition to the simple relaying mission of the relay node in the basic scenario. After presenting the signal model and the transmission rules for the network coded scenario, we give the optimal and the suboptimal network decoders for estimating the source data symbols individually and jointly as a sequence by making use of the reliability information of the network coding operations carried out at the mentioned intermediate nodes. We finally propose a heuristic improvement on the network coding procedure, which aims that the intermediate nodes avoid combining the estimated source data symbols that are not reliable enough in order to further diminish the deteriorating effects of the intermediate node errors before they propagate to the destination node.

2.1 Canonical Cooperative Network System Model

The cooperative communication system which is composed of a source, a destination and a relay node assisting these nodes is referred as the canonical cooperative communication system. This system and related fading coefficients assigned to the links between the source node S, the relay node R and the destination node D are presented in Fig. 2.1. The channel fading coefficients h_{SR}, h_{RD}, and h_{SD} are assumed to be independent and to follow zero mean circularly symmetric complex Gaussian probability distributions such that $h_{ij} \sim CN(0, \sigma_{ij}^2)$, where $(ij) \in \{SR, RD, SD\}$, nodes S and R access the channel in an orthogonal fashion according to a time-division method without loss of generality so that in the first time slot S transmits the data symbol x and nodes R and D have respective observations

$$y_{SR} = h_{SR}x + n_{SR} \text{ and } y_{SD} = h_{SD}x + n_{SD}, \tag{2.1}$$

where n_{SR} and n_{SD} denote the independent white complex Gaussian noise terms at R and D with identical distribution $CN(0, N_0)$.
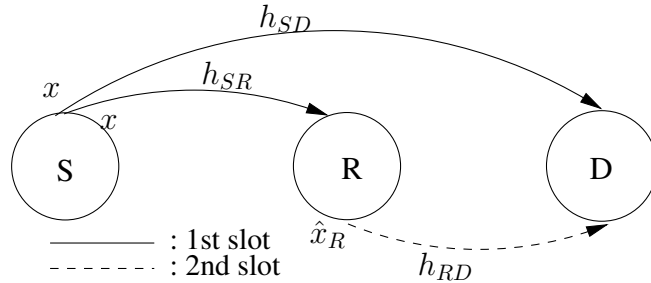
Figure 2.1: Canonical cooperative communication system

As in [46], Binary Phase Shift Keying (BPSK) is assumed for transmissions for analytical tractability with $x \in \{+\sqrt{E}, -\sqrt{E}\}$, where E is the average bit energy. Next, we define $\bar{\gamma} = \frac{E}{N_0}$ so that the instantaneous SNR values for S-R and S-D links are $\gamma_{SR} = \bar{\gamma}|h_{SR}|^2$ and $\gamma_{SD} = \bar{\gamma}|h_{SD}|^2$ respectively. These instantaneous values are exponentially distributed with respective expectations $\bar{\gamma}\sigma_{SR}^2$ and $\bar{\gamma}\sigma_{SD}^2$. When R operates as a DetF-type relay, it first detects

10

$$\hat{x}_R = \underset{x\in\left\{+\sqrt{E},-\sqrt{E}\right\}}{\arg\min} |y_{SR} - h_{SR}x|^2 \qquad (2.2)$$

and simply transmits $\hat{x}_R$, which is the optimal hard detection result for x. The observation of D after the second time slot is then $y_{RD} = h_{RD}\hat{x}_R + n_{RD}$, where $n_{RD} \sim CN(0, N_0)$ and the corresponding instantaneous SNR $\gamma_{RD} = \bar{\gamma}|h_{RD}|^2$ is also exponentially distributed.

It is given in [46] that the C-MRC method at node D has less computational complexity and is analytically more tractable with respect to the optimal detection rule. Moreover, through simulations it is shown to perform very close to the optimal rule. By using C-MRC, detection is carried out on the weighted sum of two observation signals (one directly from the source, the other over the relay). The weighting is done in accordance with the reliability of the two receptions

$$\hat{x}_D = \underset{x\in\{+\sqrt{P},-\sqrt{P}\}}{\arg\min} |w_1 y_{SD} + w_2 y_{RD} - (w_1 h_{SD} + w_2 h_{RD})x|^2, \qquad (2.3)$$

where w_1 is the weight coefficient corresponding to the $S-D$ link and is equal to h_{SD}^* as in the well-known MRC method without relaying. On the other hand, for observation y_{RD}, which corresponds to the relayed communication over the links $S-R$ and $R-D$, the coefficient w_2 should be redefined to reflect the possible error propagation on these two hops. In [46], the authors propose a single equivalent channel for representing these hops and approximate the equivalent instantaneous SNR of this channel with

$$\gamma_{eq} \triangleq \left\{Q^{-1}\left(\left[1 - P_{SR}^b\right]P_{RD}^b + \left[1 - P_{RD}^b\right]P_{SR}^b\right)\right\}^2/2, \qquad (2.4)$$

where $Q(x) = \int_x^\infty \frac{1}{\sqrt{2\pi}}\exp(-z^2/2)\mathrm{d}z$ is the well-known Q-function, Q^{-1} is the inverse Q-function, $P_{SR}^b = Q(\sqrt{2\gamma_{SR}})$ and $P_{RD}^b = Q(\sqrt{2\gamma_{RD}})$ are the instantaneous BER values for $S-R$ and $R-D$ links respectively. Accordingly we define $w_2 = \frac{\gamma_{eq}}{\gamma_{RD}}h_{RD}^*$ and using this definition R decides on the transmitted symbol using the optimal detection rule in (2.3). The instantaneous end-to-end BER expression for this detection based on the equivalent channel assumption and the C-MRC operation is derived in [46]. In Section 4.1, we start with this instantaneous BER expression and derive the expected BER expression by presenting a detailed analysis on the sampling

property [25] and proposing some generalizations on this property.

2.2 Cooperative Network Coded System Model and Design Issues

In this work, we analyze a wireless network in which unicast transmission of data symbols, each belonging to a different source, is to be carried out utilizing NC at the intermediate nodes. Under the general operation scheme, every node may act both as a member (source or destination) of a unicast communication pair and as an intermediator (relay) node for other unicast pairs. In the most general form, this network is demonstrated in Fig. 2.2, where due to practical reasons for easing the design or performance evaluation (as an example by limiting the maximum number of hops for a transmission) and/or due to spatial separation between groups of nodes, the overall network is divided into several sub-networks or *clusters*. Each one of these miniaturized networks consists of a few nodes $n_{l,i}$ where the first index l denotes the cluster number and the second index i denotes the ordering of a node in that cluster. For each cluster, one or more of the destination nodes may possibly serve as an intermediate node for conveying information to a neighbouring cluster. Furthermore, within each cluster, we assume that at most two hops are to be observed for all data transmissions for simplifying the description.

As seen in Fig 2.2, we have many clusters that are separated by thick dashed lines. In the following sections, we are going to concentrate on one of these clusters and propose some rules defining the operations of the member nodes together with corresponding decoding techniques. When we combine these proposals with the analysis techniques that we present for a cluster in Section 4, we reach a rigorous formulation for the building blocks that make up the entire wireless network coded cooperative communication system given in Fig. 2.2. This formulation is expected to supply a basis for the design and the performance analysis of the general system in the future studies in the field of NC from the communication theory point of view.

12
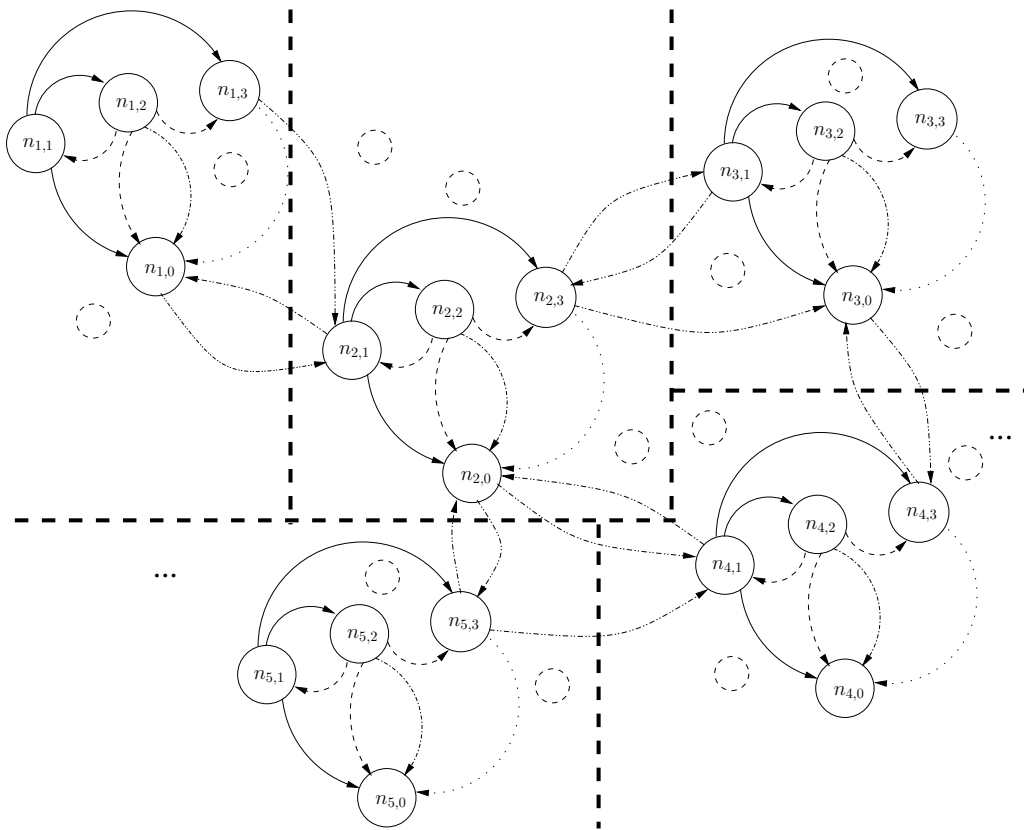
Figure 2.2: A huge network structure with many building block sub-networks.

2.2.1 The Network-Coded System Model for the Building Block Sub-Network

In order to ease the explanation of system model and the roles of nodes in the network, here we start a with a simple network-coded operation depicted for a cluster (sub-network) in Fig. 2.3, which makes use of binary NC through usual binary addition operator $\oplus$. The sub-network of interest consists of $k = 3$ source nodes and a dummy node 0. The source nodes are simply named as nodes 1, 2, and 3 by dropping the cluster index. The dummy destination node 0 represents a hypothetical detector of source packets $\mathbf{u_1}$, $\mathbf{u_2}$, and $\mathbf{u_3}$ at the corresponding destination nodes. The transmission of these 3 data packets is allowed to be completed within $n = 4$ orthogonal time slots, which form a round of NC communication with a data rate of $r = \frac{k}{n} = \frac{3}{4} \ packets/transmission \ slot$. The channel is assumed to be shared by a time division multiple access technique for the sake of simplicity in model description and due to causality requirements forcing the intermediate nodes to listen to a symbol before combining it through NC.
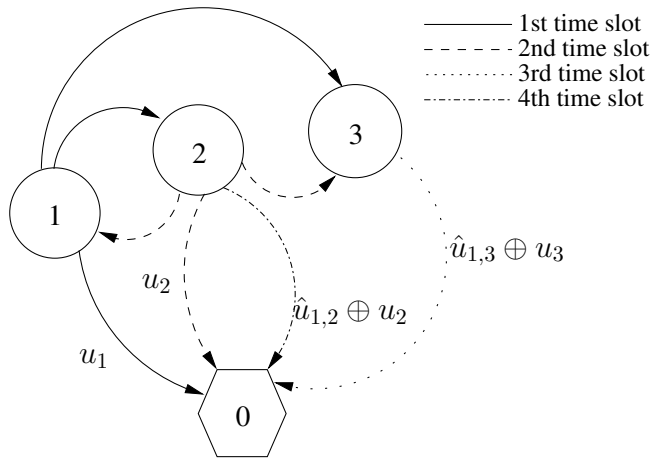
Figure 2.3: Sample network coded transmission scenario in a cluster.

As seen in Fig. 2.3, the first time slot is reserved for node 1 to transmit its own data packet $\mathbf{u_1}$ and this transmission is overheard by source nodes 2 and 3 in addition to the destination node 0. We assume that the links between different pairs of nodes are inde-

pendently Rayleigh faded. The channel corresponding to a link is quasi-static (block fading), i.e., constant over a packet and independently fading for different packets. We further assume that there is no feedback of channel state information (CSI) within the system in order to simplify the implementation. In this way, additional feedback channels that carry CSI between the nodes are avoided. This corresponds to scenario with no CSIT such that each receiving node, including node 0, has the perfect knowledge of only the incoming links through measurements of the respective channels. Hence following the transmission of the packet $\mathbf{u_1}$, both node 2 and node 3 use only their own incoming link measurements to obtain their own detection results on $\mathbf{u_1}$. Due to the block fading assumption, we consider a single data symbol u_1 and its detection/decoding event representing all symbols in the packet. Therefore, corresponding to the detections of u_1, each node has also a reliability information based on the probability of error in the detection, which is in fact only a function of its own incoming channel measurement result. In order to counteract the effects of error propagation, this reliability information is fed forward to the destination node by an intermediate node (node 2 or 3), whenever it combines the detected symbol shown by $\hat{u}_1$ with its own and other nodes' symbols.

In the second time slot, node 2 transmits its own symbol u_2 and this transmission is observed by all other nodes as well. In the following slot, a NC operation is carried out by node 3, which simply combines its own symbol and its detection result for the first time slot $\hat{u}_{1,3}$. This combination is in the form of an XOR operation for GF(2) NC and can be generalized to larger GF sizes with ease. In order to inform the destination node 0, node 3 has to append the error probability for the network coded symbol $\hat{u}_{1,3} \oplus u_3$ to the packet it formed. In the last slot, once again node 2 uses the channel to transmit the network encoded data $\hat{u}_{1,2} \oplus u_2$ which is obtained according to its own estimate of u_1 and appends the corresponding reliability information to the transmitted packet. Hence the destination node knows only the reliability information for the last two incoming transmissions which incorporate NC, but not the CSI between all intermediate nodes within the system. In this manner, the amount of CSI fed forward is kept at minimum in the network for decreasing the overhead in the packets. Moreover, for the proposed scenario, the overhead of appending a form of quantized reliability information to the network-coded packets on the spec-

tral efficiency is small for large packet lengths. Therefore, the effect of sharing the the reliability information on spectral efficiency is expected to be small. An alternative way of totally eliminating reliability information overhead in transmissions would be using the average reliability information at the destination node instead of the instantaneous ones. This method is out of the scope of this work and is only shown to result in degraded performance with NC in Section 3.3.4.

Up to this point, the sample NC system is detailed in words. From the perspective of destination node 0, the same system can be described formally using a generator matrix $\mathbf{G}$ (called the transfer matrix in [52]) and a scheduling vector $\mathbf{v}$. The columns of $\mathbf{G}$, $\mathbf{g}'_j s$, represent the combining operations at the intermediate nodes and the entries of $\mathbf{v}$ give the scheduling of the nodes accessing the channel:

$$\mathbf{G} = \begin{bmatrix} 1 & 0 & 1 & 1 \\ 0 & 1 & 0 & 1 \\ 0 & 0 & 1 & 0 \end{bmatrix}, \mathbf{v} = [1\,2\,3\,2]. \tag{2.5}$$

In (2.5), the jth column of $\mathbf{G}$ gives the network encoding to be done by the corresponding node v_j which is the jth entry of $\mathbf{v}$. Accordingly, node v_j combines the symbols of the users for which the corresponding entries in the jth column of $\mathbf{G}$ are non-zero.

The combined data vector $\mathbf{u} = [u_1\ u_2\ u_3]$ can then be used to form the distributed codeword: $\mathbf{c} = [c_1\ c_2\ c_3\ c_4] = \mathbf{u}\mathbf{G}$. The choices $\mathbf{u}$, $\mathbf{G}$, k, and n for the parameters defining the operation of network are not arbitrary. They are used intentionally to point out the analogy to regular linear block codes. However, reliable detection of all data symbols, i.e., whole block $\mathbf{u}$, originating from a single error-free source is of interest for a regular decoder; whereas node 0 may desire to reliably detect, as an example, only u_1 under cooperative encoding. Hence we need to identify a parameter that describes the performance for detection of a single symbol u_1 as opposed to the codeword $\mathbf{u}$ for our model.

One can show that the minimum distance for $\mathbf{G}$ is 1. However, we now establish that an error event requires at least 2 bit errors for decoding of u_1 at node 0. Let all the data bits be equal to 0 without loss of generality, i.e., $\mathbf{u} = [0\,0\,0]$. Hence the transmitted codeword is expected to be $\mathbf{c} = [0\,0\,0\,0]$ for the case of no intermediate

node errors. The error event for u_1 corresponds to its decoding as 1. This erroneous decoding can occur for sequence decoding $\hat{\mathbf{u}} \in \{[100], [101], [110], [111]\}$, where $\hat{\mathbf{u}}$ denotes the decoding result at node 0. The incorrect codewords $\hat{\mathbf{c}}$ corresponding to these decoded vectors are $[1011], [1001], [1110], [1100]$, respectively. When these codewords are compared to the codeword $[0000]$, it is clear that at least 2 bit errors are needed to cause an error event. Hence the minimum distance for u_1 in this setting is said to be 2. The erroneous decoding for other bits can be investigated in a similar fashion. Focusing on u_3 and hypothesizing $\mathbf{u} = [0\ 0\ 0]$, u_3 is incorrectly decoded when $\hat{\mathbf{u}} \in \{[001], [011], [101], [111]\}$. The corresponding codewords are $[0010], [0111], [1001], [1100]$. Therefore, a single bit error can cause erroneous decoding of u_3 yielding a minimum distance of 1. As for the data bit of node 2, one can find that the minimum distance is 2. As seen in the example, the error performance varies from symbol to symbol. Although unimportant from the perspective of regular codes, this differentiation of reliability may be preferred in a NC setting. Next we generalize this claim to cover arbitrary generator matrices and verify it through simulations in Sections 2.2.3 and 3.3.3.

Now we consider a subset of nodes in which there are k nodes transmitting data to a single destination node 0. Let the symbol transmitted by node i be denoted by u_i, for $i \in \{1, \ldots, k\}$, and u_i be an element from the Galois field of size q, GF(q). We assume $\{u_i\}$ to be statistically independent and define $\mathbf{u} = [u_1\ u_2\ \ldots\ u_k]$ as the combined data vector. In a given time slot $j \in \{1, \ldots, n\}$, a transmitting node $v_j \in \{1, \ldots, k\}$ forms a linear combination of its own and other nodes' data. If v_j detects all data to be encoded correctly, it simply forms $c_j = \mathbf{u}\mathbf{g}_j$, where $\mathbf{g}_j$ is a $k \times 1$ network encoding vector whose entries are elements of GF(q). Let $\hat{u}_i$ denote the estimate of the symbol of node i at node v_j. Using these estimates, node v_j forms the noisy network coded symbol $\hat{c}_j = \hat{\mathbf{u}}\mathbf{g}_j$ that is also an element of GF(q). Then v_j modulates and transmits this symbol to receiver node 0 as:

$$s_j = \mu(\hat{c}_j), \tag{2.6}$$

where $\mu(.)$ shows the mapping of a symbol to a constellation point. Although symbols may come from any alphabet and non-binary constellations may be used, we will focus hereafter on GF(2) and binary phase-shift keying (BPSK) with the mapping rule $s_j = \sqrt{E}(1-2c_j)$. Our assumption is that vector $\mathbf{g_j}$, source address v_j and probability

of error p_{e_j} for the transmitted symbol are appended to the corresponding packet. We consider transmissions with no channel coding and deal with single network coded symbol c_j which represents all symbols in a packet transmitted by v_j. At the end of a round of transmissions, if no errors occur at the intermediate nodes, the overall vector of n symbols coded cooperatively in the network is

$$\mathbf{c} = [c_1 \; c_2 \; \ldots \; c_n] = \mathbf{u} \, [\mathbf{g}_1 \; \mathbf{g}_2 \; \ldots \; \mathbf{g}_n] = \mathbf{u}\mathbf{G}. \tag{2.7}$$

The generator matrix characterizes the network code together with the vector of transmitting nodes

$$\mathbf{v} = [v_1 \; v_2 \; \ldots \; v_n]. \tag{2.8}$$

Equations (2.7) and (2.8) generalize the definition of the example NC in (2.5). Next, we present Algorithm 1, which generalizes the method for finding the minimum distance for u_i. In Algorithm 1, the function $dec2GF2(.)$ returns a binary pattern corre-

---

Algorithm 1 Algorithm for finding the minimum distance corresponding to symbol u_i for a (n, k, d) code with given generator matrix $\mathbf{G}$

$mindistance \leftarrow n$

$indexvector \leftarrow [1 \; 2 \; \cdots \; k] \setminus i$

for $j = 1$ to 2^{k-1} **do**

   $errorpattern \leftarrow dec2GF2(j - 1)$

   $errdatavector[i] \leftarrow 1$

   $errdatavector[indexvector] \leftarrow errorpattern$

   $errcodevector \leftarrow errdatavector * \mathbf{G}$

   $errdistance \leftarrow numberofnonzero(errcodevector)$

   $mindistance \leftarrow min(mindistance, errdistance)$

end for

---

sponding to the input decimal number and the function $numberofnonzero(.)$ returns the number of non-zero entries in the input vector. It is assumed that the data vector $\mathbf{u}$ consists of all zeros, relying on the linearity of the network code. The algorithm first creates all possible erroneous data vectors $\hat{\mathbf{u}}$ that have 1 in the ith position so that

all codewords leading to erroneous decoding of u_i are generated by $\hat{\mathbf{c}} = \hat{\mathbf{u}}\mathbf{G}$. Afterwards, we search within these codewords to find the one with the minimum distance to the transmitted codeword of all 0s. This minimum value gives us the minimum distance for u_i and the set of minimum distances corresponding to all u_i's (separation vector [43]) is utilized in identifying the performance metrics for different nodes under NC in Section 3.1.

2.2.2 Optimal Network Decoding Using Intermediate Node Reliability Information

The intermediate nodes are assumed to use the DetF technique (hard decision with no decoding operation) due to its simplicity. In a wireless network, an intermediate node v_j has a noisy detection result $\hat{\mathbf{u}}$ of $\mathbf{u}$. Let us express the resulting noisy network coded symbol as

$$\hat{c}_j = c_j \oplus e_j, \tag{2.9}$$

where e_j denotes this propagated error. We observe that a possible error in $\hat{\mathbf{u}}$ propagates to $\hat{c}_j$ after the NC operation dictated by $\mathbf{g}_j$ is realized. We assume that node v_j knows the probability mass function (PMF) of e_j, $p(e_j)$, which we name as the intermediate node reliability information. This assumption is not unrealistic as it can be determined by the estimation of the channel gains of the links connected to v_j, along with the reliability information forwarded to v_j. The received signal by node 0 at time slot j is $y_j = h_j s_j + n_j$, where h_j is the channel gain coefficient resulting from fading during the jth slot and n_j is the noise term for the link between v_j and node 0. The gain coefficient is circularly symmetric complex Gaussian (CSCG), zero-mean with variance 1, i.e., it has distribution $\mathbb{CN}(0, 1)$. The noise term is CSCG with $\mathbb{CN}(0, N_0)$. The usual independence relations between related variables representing fading and noise terms exist. The observation vector of length n at node 0 is

$$\mathbf{y} = \mathbf{H}\mathbf{s} + \mathbf{n}, \tag{2.10}$$

where $\mathbf{y} = [y_1 \ \ldots \ y_n]^T, \mathbf{s} = [s_1 \ \ldots \ s_n]^T = \mu(\hat{\mathbf{c}}^T), \mathbf{n} = [n_1 \ \ldots \ n_n]^T$ and $\mathbf{H}$ is a diagonal matrix whose elements are independent and perfectly known channel gains $h_1, h_2, \ldots, h_n$ for the links connected to node 0. Combining the coded symbols in a

19

network code vector, we obtain

$$\hat{\mathbf{c}} = \mathbf{c} \oplus \mathbf{e} = \mathbf{u}\mathbf{G} \oplus \mathbf{e}, \tag{2.11}$$

where $\mathbf{e} = [e_1 \ \ldots \ e_n]$ is the error vector denoting the first hop errors. We assume that $\mathbf{e}$ is independent of $\mathbf{c}$ although dependence can be incorporated in the SP decoder developed in Section 3.3. This independence assumption is valid directly for BPSK modulation, whereas in a general modulation scheme the Euclidean distances between various constellation point pairs differ and an error term e_j depends on the symbol being transmitted. Although this dependence may be eliminated by use of well-known Bit Interleaved Coded Modulation (BICM) technique [10] through interleaving, this issue is kept out of the scope of the work here. As a result, using (2.9), (2.10), and (2.11), we have

$$\mathbf{y} = \mathbf{H} \, \mu(\mathbf{u}\mathbf{G} \oplus \mathbf{e})^T + \mathbf{n}. \tag{2.12}$$

Thus node 0 has access to the likelihood $p(\mathbf{y}|\mathbf{u}, \mathbf{e})$ and $p(\mathbf{e}) = \prod_{j=1}^{n} p(e_j)$, assuming the errors are independent. As shown in [11], in order to avoid the propagation of errors occurring at intermediate nodes, node 0 has to utilize the reliability information $p(\mathbf{e})$. Then, the a posteriori probability of a source bit, say u_1, is calculated by using the Bayes' rule:

$$p(u_1|\mathbf{y}) = \alpha \sum_{u_2,\ldots,u_k} \sum_{e_1,\ldots,e_n} p(\mathbf{y}|\mathbf{u}, \mathbf{e}) \prod_{j=1}^{n} p(e_j), \tag{2.13}$$

where α is a constant that does not depend on u_1. The MAP estimate of u_1 at node 0 is denoted by $\hat{\hat{u}}_1$ and obtained as

$$\hat{\hat{u}}_1 = \arg\max_{u_1} p(u_1|\mathbf{y})$$

$$= \arg\max_{u_1} \sum_{u_2,\ldots,u_k} \sum_{e_1,\ldots,e_n} p(\mathbf{y}|\mathbf{u}, \mathbf{e}) \prod_{j=1}^{n} p(e_j), \tag{2.14}$$

which is the *individually* optimum detector for u_1. The *joint* MAP rule detecting the sequence $\mathbf{u}$ as a whole may also be preferable in terms of computational complexity and ease of analysis:

$$\hat{\mathbf{u}} = \arg\max_{\mathbf{u}} \sum_{e_1,\ldots,e_n} p(\mathbf{y}|\mathbf{u}, \mathbf{e}) \prod_{j=1}^{n} p(e_j). \tag{2.15}$$

20

The jointly optimal detector given in 2.15 is in fact the detector that we base our minimum distance discussion on in Section 2.2.1. Hence although it is suboptimal, it achieves the maximum diversity orders for all nodes in the network just as the individually optimal detector presented in 2.14. As a result, for both the optimal individual and joint detection of u_1, node 0 requires the intermediate node reliability information vector: $\mathbf{p_e} = [p_{e_1} \ \ldots \ p_{e_n}]$, where $p_{e_j} = P(e_j = 1)$ depends on the PMF of e_j. These reliability values are hence assumed to be appended to the data packets generated at the intermediate nodes. One final note ought to be made on the use of the detection rules given in 2.14 and 2.15 for the case of a conventional communication technique without NC such that each source node repeats its own data for a given number of time slots. In this case for all time slots, $j = 1, 2, \ldots, n$, the error terms are deterministically zero, $e_j = 0$. Moreover, the source bits are not combined through NC and hence each observation is dependent on a single source bit and independent of other source bits. In this way, both the individually and the joint optimal detections rules for a source bit, as an example u_1, are simplified to

$$
\begin{aligned}
\hat{\hat{u}}_1 &= \arg\max_{u_1} \prod_{j:v_j=1} p(y_j|u_1) \\
&= \arg\max_{u_1} \left| \sum_{j:v_j=1} h_j^* y_j - \sum_{j:v_j=1} |h_j|^2 u_1 \right|,
\end{aligned}
\tag{2.16}
$$

which is the Maximal Ratio Combining (MRC) type detector with weighted observations corresponding to the transmissions done by node 1. We observe the performance of these detection rules for both NC and repetition type transmissions in Section 2.2.3.

The problem related to the MAP-based detection rules of (2.14) and (2.15) is the number of required operations, which grows exponentially both in the number of nodes k and the number of possible error events n. This is addressed in Section 3.3, where we suggest a practical network decoding technique.

2.2.3 Sample Network-I: Simulation Results

The results in this section are based on Sample Network-I described in (2.5), consisting of 4 nodes, to observe the fundamental issues. At least 100 bit errors for each data bit u_1, u_2, and u_3 are collected through simulations for each SNR value. In each

run, data bits, intermediate node errors and complex channel gains are randomly generated with their probability distributions. The solid lines in Fig. 2.4 show the BER values for the optimal detector operating under the realistic scenario of intermediate node errors, whereas the dashed lines depict the performance of the genie-aided no-intermediate-error network with the same optimal detection. This latter cased is therefore named as "perfect relaying" on the legend.
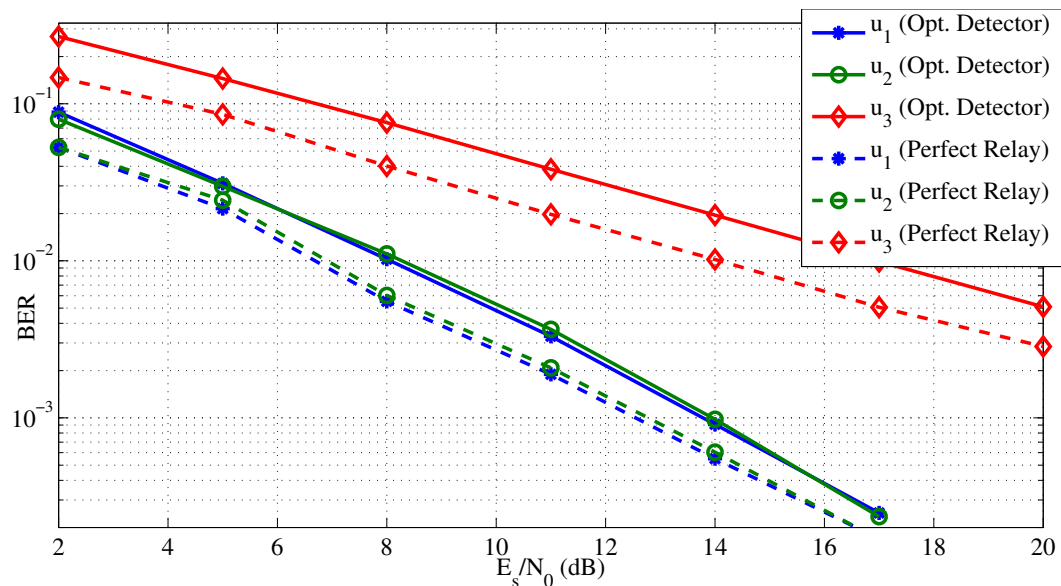
Figure 2.4: BER performance for different nodes under optimal detection with intermediate node errors and with a hypothetical scenario of no intermediate node errors

It is observed in Fig. 2.4 that different diversity orders for bits of different nodes are apparent for optimal detection under intermediate errors. The diversity order for u_1 is observed to be 2 according to the slope of the corresponding BER curve. This is in agreement with the analytical results in Section 2.2.1 where it is shown that an error event corresponds to at least 2 bit errors for the detection of u_1 and u_2. It is seen in Fig. 2.4 that the intermediate node errors cause no loss of diversity for u_1 and u_2, but an SNR loss of 1.5 dB due to the decreased coding gain. Hence the optimal detection rule of (2.14) is said to avoid the problem of error propagation in terms of the diversity orders. The loss for u_3, whose diversity order is 1, with respect to the hypothetical no-intermediate-error network is around 3 dB.
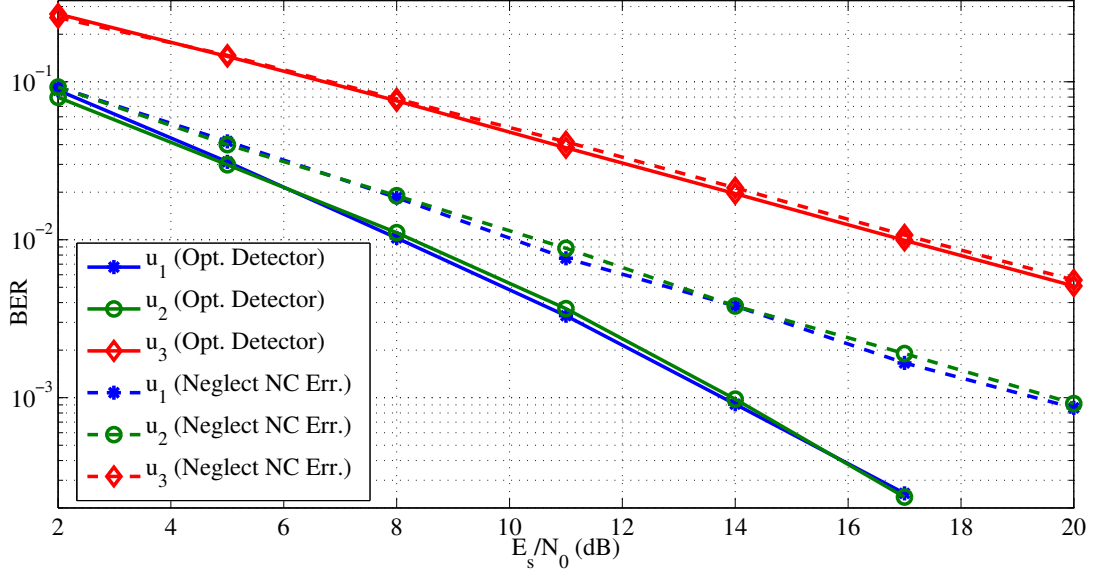
Figure 2.5: BER performance for different nodes under optimal detection with intermediate node errors and detection with neglecting the intermediate node errors

In Fig. 2.5 the dashed lines are for the detector that totally neglects intermediate errors, which corresponds to the scenario where the receiver assumes that all network coded data bits in the network are correct. The performance deteriorates significantly for especially u_1 and u_2 when intermediate errors are neglected in detection, i.e., $p_{e_3} = p_{e_4} = 0$ is assumed. Not only an SNR loss is endured but also the diversity gains due to use of NC disappear.

One final note on Sample Network-I would be related to the suboptimal (jointly optimal for the sequence) detection rule given in (2.15). Through simulations we have observed that the SNR loss endured by using this rule with respect to the optimal rule presented by (2.14) is clearly negligible (less than 0.1 dB) for a set of BER values ranging from 10^{-1} to 10^{-4} for Sample Network-I and also for many other larger networks. Therefore, we do not present any figures for comparison of these two detection rules in this work.

2.2.4 Selective Network Coding

The NC described in Section is a static method in the sense that the generator matrix $\mathbf{G}$ is fixed. In static NC, node v_j always combines (network encodes) the symbols of a pre-determined set of users, even when it knows that the reliability for one of those users is low. When a symbol estimate with low reliability is combined with a symbol with high reliability, the reliability of the resulting network coded symbol is low. Thus, it is intuitive to expect some gains in performance by forcing the intermediate nodes not to combine the symbols that have very low instantaneous reliability. In [18] and [38], various forms of channel state information are used to fix thresholds for relaying decisions. In [52] and [37], for relays assuming DF operation, successful decoding of channel code for a source is the condition for combining its data in NC. Here, we propose a method called Selective Network Coding (SNC) that imposes a threshold on the reliability of the candidate symbols to be encoded at intermediate nodes that adapt DetF. In this way, any symbol that is sufficiently reliable is included in network encoding and the resulting encoding vector $\mathbf{g}_j$ is appended to the transmitted packet so that node 0 still has the instantaneous generator matrix $\mathbf{G}$ at the end of n transmissions.

Let us demonstrate the operation under SNC on the sample network given in Fig. 2.3. For the first two time slots SNC is equivalent to NC since no combining of other nodes' symbols is the case. However, in the third slot, node 3 checks the reliability of the detection for u_1 carried out following the first slot. Let us say it has observed an instantaneous SNR value on the link from node 1 to 3 that is equal to $\gamma_{1 \to 3}$, which is measured by node 3. This yields a probability of error $p_{e_3} = Q(\sqrt{2\gamma_{1 \to 3}})$ in detection of u_1 for BPSK modulation. Here, the Q-function is defined as $Q(x) = \frac{1}{\sqrt{2\pi}} \int_x^\infty exp(-\frac{z^2}{2}) \mathrm{d}z$ and the random variable $\gamma_{1 \to 3}$ is exponentially distributed with mean value equal to average SNR $\bar{\gamma}$ for a Rayleigh fading channel. Although many other ways of setting a threshold on the reliability exists, we exemplify the technique by using the error probability p_{e_3} as a measure of reliability for $\hat{u}_1$ and average it over

the distribution of $\gamma_{1\to3}$ to set a threshold:

$$p_{th_3} = \int_0^\infty Q(\sqrt{2\gamma_{1\to3}})\frac{1}{\bar{\gamma}}\exp\left(-\frac{\gamma_{1\to3}}{\bar{\gamma}}\right)\mathrm{d}\gamma_{1\to3}$$
$$= \frac{1}{2}\left(1 - \sqrt{\frac{\bar{\gamma}}{1+\bar{\gamma}}}\right), \tag{2.17}$$

which is the expectation operation over $\gamma_{1\to3}$. We should also mention that after conducting extensive simulations on various networks, we have observed that this method of setting the threshold as the expected value of the reliability of the corresponding links is very close to the optimal selection that minimizes the BER value. Therefore, node 3 uses the threshold value p_{th_3} to check whether the detection at that instant is reliable. If $p_{e_3} < p_{th_3}$, the detection is decided to be reliable enough and the combination $\hat{u}_1 \oplus u_3$ is formed just in the way declared by the generator matrix $\mathbf{G}$. Otherwise, node 3 modulates and transmits only its own symbol u_3 and appends this information to the corresponding packet. Similarly, in the last slot, node 2 checks the reliability of its own detection of u_1 and forms either $\hat{u}_1 \oplus u_2$ or simply transmits u_2. Here, the reliability of $\hat{u}_1 \oplus u_2$ is equal to the reliability of $\hat{u}_1$. In general, there may be more than one symbol that an intermediate node should detect and combine according to $\mathbf{G}$. In such cases the combined instantaneous reliability of an network encoded symbol at the time slot j can be easily obtained by

$$p_{e_j} = \frac{1 - \prod_{i\in A_j}\left(1 - 2P_j(\hat{u}_i \neq u_i)\right)}{2}, \tag{2.18}$$

where A_j denotes the set of sources for which v_j should carry out the network coding, i.e., A_j is the set of indices corresponding to the non-zero elements of the jth column of $\mathbf{G}$, $\mathbf{g}_j$. The term $P_j(\hat{u}_i \neq u_i)$ in (2.18) is used to show the probability of error for detection of u_i by node v_j. In Sample Network-I, when we consider the AWGN signal disturbing the observation at node v_j, we find that $P_j(\hat{u}_i \neq u_i) = Q\left(\sqrt{2\gamma_{i\to v_j}}\right)$ with given SNR value $\gamma_{i\to v_j}$ for the link from node i to v_j in the time slot that node i transmits its own data u_i. As a result, each intermediate node calculates its network encoding reliability p_{e_j} by making use of only the incoming links' CSI and then forwards this calculation result to the destination as a single quantized value.

Clearly, SNC inherently includes usage of adaptive generator matrices. The utilized generator matrix may assume in average a form dictated by some predetermined (and optimal if possible) linear block code structure like the ones that are to be discussed

in Section 3.2. However, we should stress that there are many other ways of letting a network of nodes randomly coding their data in a distributed fashion, which requires a more detailed code construction methodology and optimization of many parameters (thresholds and number of packets to be combined at each intermediate node). These latter issues are not in the scope of this work, only a special case (SNC) is investigated. The bit error rate (BER) performance improvements owing to the use of this random NC technique are observed in Section 3.3.4.

2.3   Discussion

We present the system model for the basic cooperative communication scenario in this section. It includes single DetF-type relay assisting a source node which also reaches the destination node through a direct link. The equivalent channel approach and the C-MRC method that ease the analysis of this scenario in Section 4.1 is described. This is followed by the NC system model which can be seen as the generalization of the canonical scenario. This NC model includes intermediate nodes which are also source nodes in addition to their relaying capability of more than one source symbols simultaneously thanks to the distributed coding functionality assigned to them. This assignment is formalized via the definition of the generator matrix and scheduling vector definitions that uniquely identify the operations of a NC system. The algorithm to obtain the error protection levels provided to different nodes is also given in this section.

It is shown that the intermediate node coding reliability information is essential for the individually and jointly optimal network decoding rules for the proposed system. The close BER performance of these two decoders in addition to the comparison to a genie-aided no-intermediate node error system are obtained via simulations. Both of these rules are evaluated to satisfy the maximum achievable diversity order by avoiding the error propagation at the destination side.

Also we further improve the NC system model by suggesting a simple control mechanism to be implemented at the intermediate nodes: selective network coding (SNC). In this way, the combining of assisted packets is made conditionally based on a reli-

ability threshold. Untrusted packets are avoided to be combined with the expectation that the propagation of errors due to intermediate node operations is decreased. Fulfilling this expectation, we observe improvements in coding gain for each data bit in the network as to be given in Section 3.3.4.

One final note is that the NC signal model and the corresponding detection rules detailed in this section should be generalized for adaptation to the entire network of many clusters presented in Fig. 2.2. This can be accomplished by considering the destination nodes of each cluster as the intermediator nodes for the neighbouring clusters responsible for conveying information further. The detection results of such a node are then attached reliability values which have to be forwarded together with data packets within the network just as a generalization of the scenario discussed in this section.

CHAPTER 3

NETWORK CODE CONSTRUCTION AND SUM-PRODUCT ALGORITHM BASED LOW-COMPLEXITY DECODING

In this section, we establish the methodology for constructing network codes by describing the basic parameter as the diversity order assigned to each node. We give some clues on obtaining the diversity orders assigned to distinct nodes by discussing the linear block codes that form the basis for the distributed network codes. This idea is exemplified via a family of close-to-optimal linear block codes that are known as greedy codes. Again by using greedy codes, we present results on the asymptotic superiority of NC in terms of rate versus diversity trade-off and the rate advantage in comparison to the conventional method of repeating the data packets in given time slots without NC. In addition to these infinite-SNR theoretic results, we show the superiority of NC for a practical scenario of $n = 4$ nodes in terms of end-to-end BER performance simulations.

The computational complexity burden of the optimal and suboptimal decoder structures described in Section 2.2.2 is reduced by a novel network decoder based on the SP algorithm iterating on a Tanner graph that we develop for our specific NC scenario. Then, we show nearly optimal BER performance of this SP decoder. Moreover, in this section, we also provide performance improvement obtained by using the SNC described in Section 2.2.4. In doing this, we also make use of various greedy codes and SP decoding.

The final issue that is briefly discussed in this sections is the investigation of the gains that are to be obtained by using NC under slow fading channels, which have coherence durations on the order of several packets. From this preliminary results,

we reach the idea that NC would be even more fruitful due to its potential to create diversity opportunities via assisting intermediate nodes under such a setting.

3.1 Using the Separation Vector as a Performance Metric for NC

Our goal is now to explore the error performance metrics for network coding/decoding described in Section 2.2. Our basic figure of merit will be the diversity order corresponding to the source bit u_i, which is an asymptotic term defined for SNR tending to infinity:

$$d_i = -\lim_{SNR \to \infty} \frac{\log P_{\hat{u}_i \neq u_i}(SNR)}{\log SNR} \tag{3.1}$$

giving information on the slope of reliability vs SNR in log-log scale for high SNR values. For conventional block coding, the average error performance over all data symbols is of interest. Therefore, for a linear block code whose coded symbols are transmitted over independent channels, the metric utilized for comparison is the minimum distance, which is equal to the diversity order [39]. On the other hand, there is a vector of distinct minimum distances, i.e, separation vector, for data symbols, whenever we are interested in performance of individual symbols that originate from different source nodes. According to the results presented for suboptimal decoders in [14, 20], the diversity orders for symbols in some sample NC systems are still equal to the minimum distances in the corresponding separation vector in spite of the inherent error propagation problem. Using the soft decoding that we propose in (2.14) and also authors analyze in [21], one should expect better performance and consequently diversity orders being equal to the minimum distances. A similar result is also shown for a simpler cooperative network with possible relay errors and the use of *equivalent channel* defined as the combination of the source-to-relay and the relay-to-destination channels [46]. In [46], even a suboptimal detection rule utilizing this equivalent channel approach is shown to attain the achievable diversity order. As a result, supported with intermediate node reliability information, the optimal rule of (2.14) given in Section 2.2.2 also satisfies the diversity orders dictated by the separation vector whose entries are obtained according to Algorithm 1. Furthermore, by generalizing the analysis made for identifying the end-to-end BER performance for

30

Sample Network-I in Chapter 4, one can also reach the result that the minimum distance values resulting from the generator matrix directly give us the corresponding diversity orders.

It should be also noted that since diversity order is an asymptotic quantity, the exact form of $\mathbf{v}$ is irrelevant to the procedure used for obtaining a diversity order value. On the other hand, it is wiser that each column $\mathbf{g_j}$ of $\mathbf{G}$ is used as the encoding function for a v_j such that the jth entry is non-zero, $\mathbf{g_j}(v_j) \neq 0$. Otherwise possibly an extra relaying error is also included in the encoded data symbol. Therefore, $\mathbf{v}$ clearly affects the coding gain corresponding to the BER versus SNR curve of u_i.

3.2   An Example of Close-to-Optimal Linear Block Codes: Greedy Codes

In this study, we make use of some well-known linear block codes while constructing network codes that are to be used for the analysis of data rate and diversity orders for distinct symbols in Section 3.2.1 and simulation of BER in Sections 3.2.2 and 3.3.4. However, the cooperative network coding described in this work and the resulting performance figures for a unicast pair are more general and applicable to any linear block code like the maximum distance separable (MDS) codes detailed in the context of NC in [52].

In comparison with the network coded operation, we consider a case with no distributed coding (no network coding) among the nodes. For this no network coding scenario, we should also consider that our system model does not allow feedback of CSI within the network and that the average SNR values between all nodes are equal. If one intends to achieve higher diversity orders, two resources are available in such a scenario: (i) the temporal diversity resources over the faded blocks, (ii) the spatial diversity resources over the intermediate nodes. Here, it is seen that the source nodes must simply repeat their data instead of choosing a relay to convey their data which may possibly inject errors leading to worse performance than repetition. In conclusion, we call this method as the repetition coding scheme which is in fact a degenerate NC scheme with no cooperation hence with reduced spatial diversity resources. Moreover, this repetition method is also thought to be a good representative

31

for the ARQ error control mechanism utilized in many data transmission systems. In fact, with the repetition coding method, the destination node decides on data bits by combining all observations different than ARQ, which considers only the latest observation. In this way, after n transmissions are completed, node 0 combines the data received for each source symbol to optimally detect them.

On the other hand, with NC, we take the family of block codes known as greedy codes as an example. These (n, k, d) codes are selected with the following parameters: blocklength (number of transmission slots) n, dimension (number of unicast pairs) k, and minimum distance (minimum diversity order) d. Greedy codes are known to satisfy or be very close to the optimal dimensions for all blocklength-minimum distance pairs [9] and can be generalized to non-binary fields [34] for achieving higher diversity orders with NC as discussed in [52]. Moreover, they are readily available for all dimensions and minimum distances unlike some other optimal codes. Hence, even in an ad hoc wireless network with time-varying size, any desired diversity order can be flexibly satisfied by simply broadcasting the new greedy code generator matrix $\mathbf{G}$ to be utilized in subsequent rounds of communication.

As an example, consider a network that consists of $k = 3$ nodes transmitting their symbols over GF(2). If a round of communication is composed of $n = 6$ transmissions, we deal with codes of type $(6, 3, d)$, which have a code rate of $\frac{1}{2}$ bits/transmission. Starting with the generator matrix and scheduling vector corresponding to the repetition coding, we have

$$\mathbf{G} = \begin{bmatrix} 1 & 0 & 0 & 1 & 0 & 0 \\ 0 & 1 & 0 & 0 & 1 & 0 \\ 0 & 0 & 1 & 0 & 0 & 1 \end{bmatrix}, \mathbf{v} = [1\,2\,3\,1\,2\,3]. \tag{3.2}$$

It is easily observed that, since each data bit is transmitted twice over independent channels, this method satisfies only a diversity order of 2 for all bits u_1, u_2, and u_3. In contrast, a diversity order of 3 for all sources can be achieved using NC, with the same code rate. As an example, the NC that achieves this performance can be

obtained using the $(6, 3, 3)$ greedy code, as follows:

$$\mathbf{G}_1 = \begin{bmatrix} 1 & 0 & 0 & 1 & 1 & 0 \\ 0 & 1 & 0 & 0 & 1 & 1 \\ 0 & 0 & 1 & 1 & 0 & 1 \end{bmatrix}, \mathbf{v}_1 = [1\,2\,3\,1\,2\,3]. \tag{3.3}$$

Clearly, without NC, the diversity order of 3 for all sources can only be achieved with rate $\frac{1}{3}$ bits/transmission. It should also be noted that greedy codes accommodate each unicast pair with equal diversity order due to the greedy algorithm utilized in their construction. Moreover, contrary to the findings in [52], it is easy to obtain any required diversity order for any data bit even by using GF(2). The limitation is not due to the number of unicast pairs but due to the number of transmission slots in general. By increasing n, one can arrange and improve the diversity orders, if the transmissions to each node are realized over independent channels, which is a natural assumption for many wireless communication scenarios. If we need an increase in data rate, through a trade-off mechanism, we can assign decreased diversity orders to the lower-priority unicast pairs by omitting some columns of a greedy code generator matrix in order to decrease number of transmissions. The columns to be excluded can be decided by running Algorithm 1 in Section 2.2.1 on candidate punctured generator matrices. As an example, the following punctured $(5, 3, 2)$ code is obtained by omitting the last column of $\mathbf{G}_1$ and has a data rate $\frac{3}{5}$ bits/transmission that is higher than those of above two codes:

$$\mathbf{G}_2 = \begin{bmatrix} 1 & 0 & 0 & 1 & 1 \\ 0 & 1 & 0 & 0 & 1 \\ 0 & 0 & 1 & 1 & 0 \end{bmatrix}, \quad \mathbf{v}_2 = [1\,2\,3\,1\,2]. \tag{3.4}$$

The punctured network code in (3.4) satisfies a diversity order of 3 for u_1 and an order of 2 for both u_2 and u_3. If u_1 is of higher priority, this unequal error protection would be preferable especially when the higher rate of the code is considered. In case of a larger diversity order need, $d = 4$ as an example, we may utilize the $(7, 3, 4)$ greedy code with rate $\frac{3}{7}$ bits/transmission.

$$\mathbf{G}_3 = \begin{bmatrix} 1 & 0 & 0 & 1 & 1 & 0 & 1 \\ 0 & 1 & 0 & 0 & 1 & 1 & 1 \\ 0 & 0 & 1 & 1 & 0 & 1 & 1 \end{bmatrix}, \mathbf{v}_3 = [1\,2\,3\,1\,2\,3\,1]. \tag{3.5}$$

A final problem is the selection of vector $\mathbf{v}$. Our basic assumption is that $\mathbf{v}$ satisfies causality so that no intermediate node v_j tries to transmit another node's symbol before hearing at least one copy of it. This causality problem can be solved trivially by using only systematic generator matrices. For the transmitting nodes corresponding to the non-systematic part of $\mathbf{G}$, as described in Section 3.1, one can select each entry v_j such that $\mathbf{g_j}(v_j) \neq 0$ for each column $\mathbf{g_j}$. For the columns that have more than one non-zero entry, a random selection between candidate v_j's will merely affect the coding gains assigned to these nodes. As a result, one can force the number of transmissions of each node within a round to be equalized as much as possible for similar coding gain improvements of nodes. Another approach to the problem would be selection of the scheduling vector adaptively within in a session of communication. This makes sense particularly in a practical scenario where in the first few slots the data for a source node is conveyed to the destination with very high reliability so that the remaining nodes should use the channel in the subsequent slots for improving the reliability of the remaining data bits. Hence in general, a work with focus on the selection of the scheduling vector may be interesting.

In the way exemplified in this section, one can choose a network code satisfying desired error protection properties for a given network size with adequate data rate quite flexibly. This property is used in the following section for theoretical analysis of the gains obtained by utilizing NC.

3.2.1 Theoretical Gains in Rate and Diversity for NC

In this section, we investigate the rate and diversity (asymptotic) gains of NC through use of the family of greedy network codes detailed in Section 3.2, although the results are still valid for any other family of optimal or close-to-optimal codes. The availability of a greedy code for a given (k, d) pair is checked using [27]. Fig. 3.1 shows the diversity gains attainable using greedy NC (with punctured codes in case no corresponding greedy code exists) with respect to the repetition coding scenario. We define the rate in terms of information packets transmitted per time slot or equivalently the information bits transmitted per symbol transmission in the channel. In that way, the rate for a given network code constructed for k users and n transmissions

is calculated as $r = \frac{k}{n}$. The rate-diversity trade-off curves of both cases are plotted for a network of $k = 3$ nodes with increasing number of transmissions and hence decreasing rate. We are interested in three types of network diversity orders; average, minimum and maximum, since the orders corresponding to each one of the three nodes may be unequal in general. The curves with no markers represent the (average) network diversity orders for both scenarios, which is defined as the arithmetic mean of orders for three nodes. For $n = 7$, the rate is $\frac{3}{7} = 0.43$ bits/transmission for the $(7, 3, 4)$ greedy code obtained from [27]. In turn, due to symmetric construction of greedy codes; the minimum, maximum, and average diversity orders are equal for this case and all three nodes observe a diversity order equal to 4. Hence, the network diversity order for this NC scenario is 4. In contrast, the repetition scheme results in an average order of nearly 2.33 with the worst node observing a minimum order of 2 and the best node a maximum order of 3, which would mean a high SNR loss asymptotically for all three nodes in the network.
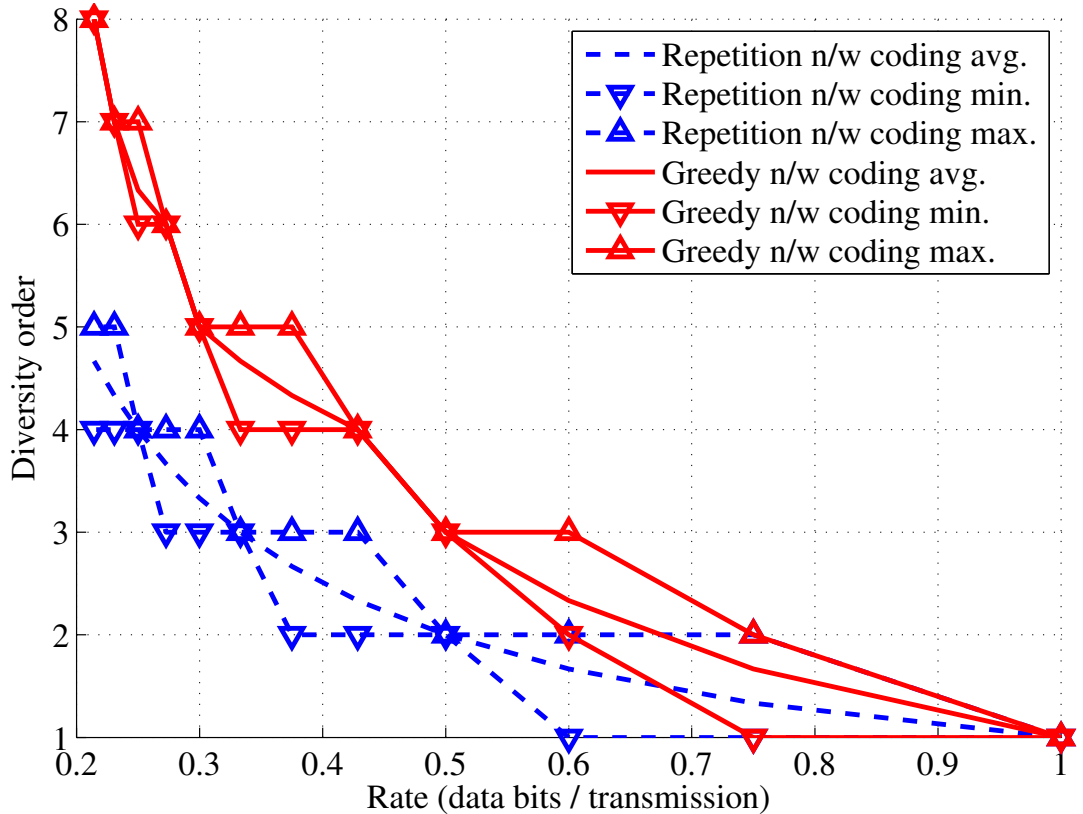
Figure 3.1: Network diversity orders: Greedy NC and repetition coding.

In Fig. 3.2, we now fix the desired network diversity order to $d = 3$ and observe the rate advantage of the NC for increasing network size. Note that for all cases diversity orders for k users are equal to 3. For a network of $k = 25$ nodes, the rate with NC is $\frac{25}{30}$ bits/transmission (with greedy code $(30, 25, 3)$) and the rate of the repetition scheme is $\frac{15}{45}$ bits/transmission (always equal to $\frac{1}{3}$ for a diversity order of 3). The rate advantage ratio is then 2.5. In the asymptotic case, as $k \to \infty$ and hence as $n \to \infty$, NC using optimal codes in construction will have a rate advantage converging to 3 since the rate for network coded case can be shown to tend to 1 using the Gilbert-Varshamov bound [48]. In general, the rate advantage of NC over the repetition scenario becomes simply d, the desired network diversity order. As a result, increasing the network size improves the network coded system's efficiency in comparison to the repetition coding.
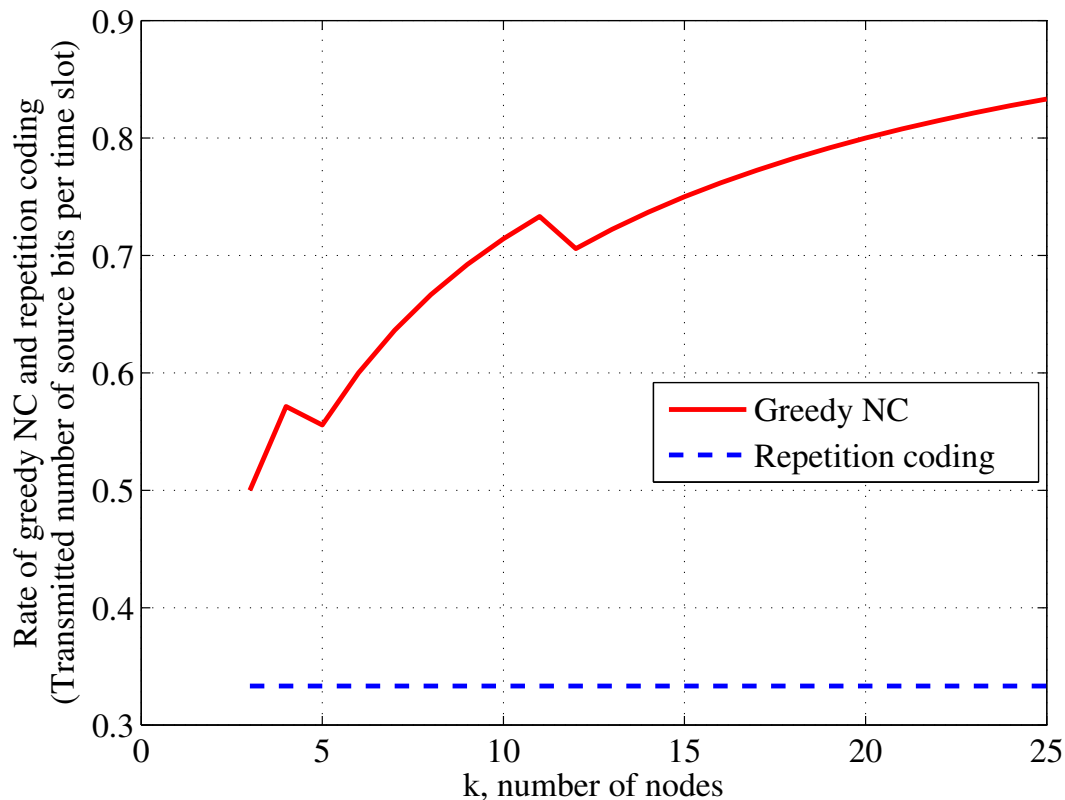
Figure 3.2: Rate advantage of greedy NC for increasing network size.

3.2.2 Sample Network-II with Greedy Codes: Simulation Results

Next, we verify the analytical results concerning the diversity orders for a set of three nodes operating under three different network codes constructed in Section 3.2. Moreover, the unequal error protection performance of one of these codes is identified together with the rate advantage it provides.

Repetition method is represented by $\mathbf{G}$ and $\mathbf{v}$ in (3.2). To construct Code-1 and Code-2, we make use of the greedy code of (3.3) and the punctured greedy code of (3.4) respectively. Fig. 3.3 exhibits the BER curves for the repetition scenario with $n = 6$ transmissions (dashed lines), for NC scenarios with Code-1 with $n = 6$ (solid lines) and Code-2 with $n = 5$ (dotted lines). The optimal detector of (2.14) is utilized for this simulation. Clearly, Code-1 has superior performance with an average network diversity order of 3. However, the lower rate of Code-1 (and also repetition coding) in comparison to Code-2 should also be noted. For Code-2, on the other hand, bits u_2 and u_3 observe a diversity order of 2 while u_1 observes an order of 3. With this unequal protection in mind, the average network diversity order for Code-2 is $\frac{2+2+3}{3} \simeq 2.33$, which is higher than that of the repetition coding with order 2. In addition to improved diversity, Code-2 has also the advantage of increased overall rate and decreased decoding delay due to usage of 5 slots instead of 6. It is preferable particularly for a network that puts higher priority on u_1 than other two nodes' data and have stricter delay constraints.

3.3 Sum-Product Network Decoder

3.3.1 Sum-Product Algorithm for Decoding LDPC Codes

This section gives introductory information on the message passing and the message initialization rules used for decoding the well-known family of LDPC codes. In the literature, SP decoding (or more generally message passage decoding) has been shown to perform quite close to the Shannon's capacity limit [40] when utilized on the bipartite graphs that are constructed for low-density parity-check (LDPC) codes [15, 33]. These bipartite graphs represent the connections between the variable
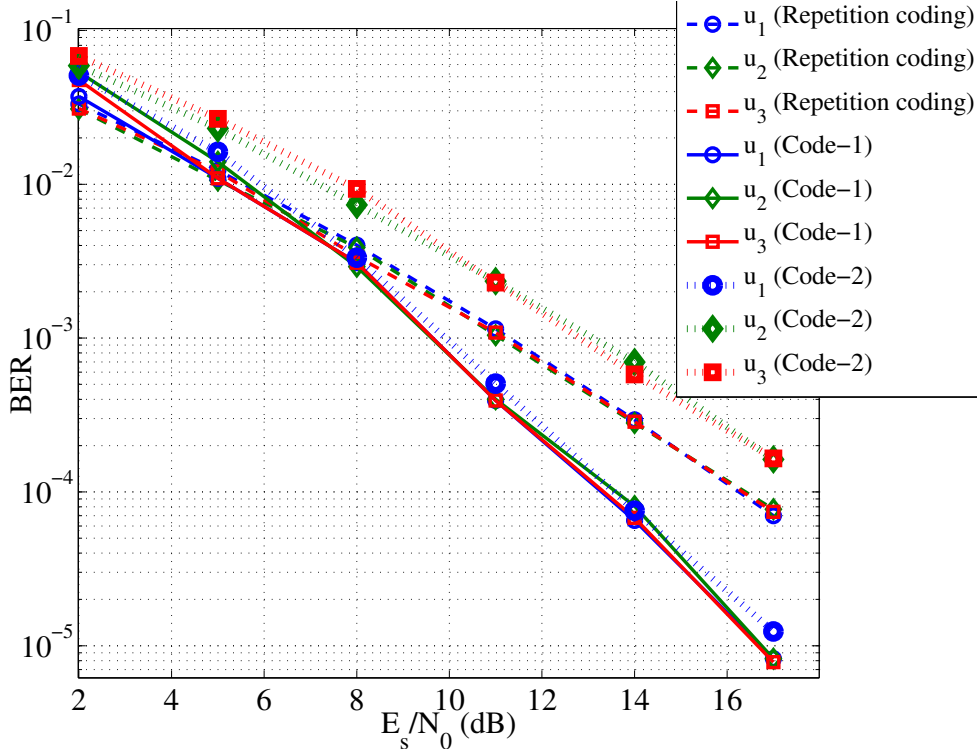
Figure 3.3: BER performance for repetition coding and greedy NC.

nodes that originate from the codeword bits and the check nodes that take roots from the parity check constraints of the LDPC codes. Another common naming for these graphs over which the conditional probability information (messages) are passed iteratively is Tanner graphs due to [42].

In the context of LDPC decoding via sum-product (SP) algorithm, the messages that are passed are usually the conditional probabilities of the bits to be decoded and for easing the calculations they are stored as the log-likelihood ratio (LLR) values. As an example the LLR corresponding to a codeword bit c_i is defined as

$$\text{LLR}(c_i) = \log\left(\frac{\Pr\left(c_i = 0 | \text{channel output for } c_i\right)}{\Pr\left(c_i = 1 | \text{channel output for } c_i\right)}\right). \tag{3.6}$$

The LLR values for the codeword bits are input to the LDPC decoder, which carries out iterations on the Tanner graph that is also input to the decoder in the form of a parity check matrix for the given LDPC code. Within each iteration, firstly the messages to be conveyed from the check nodes to the variable nodes r_{ji} are updated

according to the following rule.

$$\text{LLR}(r_{ji}) = 2 \text{ atanh} \left(\prod_{i' \in V_j \setminus i} \tanh \left(\frac{\text{LLR}(q_{i'j})}{2} \right) \right), \tag{3.7}$$

where $\text{LLR}(q_{i'j})$ is the message that is conveyed from the variable node i' to the check node j in the previous iteration step and V_j is the set of variable nodes that are connected to the same check node. For the first iteration all $\text{LLR}(q_{ij})$ values are initialized to the $\text{LLR}(c_i)$ values input to the decoder. Secondly, the messages from the variable nodes to the check nodes q_{ij} are updated according to the new values found in (3.7) as

$$\text{LLR}(r_{ji}) = \text{LLR}(c_i) + \sum_{j' \in C_i \setminus j} \text{LLR}(r_{j'i}), \tag{3.8}$$

where C_i is the set of check nodes that are connected to the variable node i. Following a previously determined number of iteration on the equations (3.7) and (3.8), the intrinsic LLR values for the codeword bits are calculated at the end as follows:

$$\text{LLR}(Q_i) = \text{LLR}(c_i) + \sum_{j' \in C_i} \text{LLR}(r_{j'i}). \tag{3.9}$$

At the output of the SP decoder, if the hard decision results are required, c_i is estimated as 0 if $\text{LLR}(Q_i) > 0$ and 1 otherwise.

3.3.2 Extension of Sum-Product Algorithm to Tanner Graph of a Network Code

The complexity of the optimal rule for decoding of any unicast transmission symbol u_i grows exponentially, since the number of additions and multiplications in (2.14) increase exponentially in the number of users and transmissions. Therefore, this rule becomes inapplicable even for moderate-size networks. Recently the SP iterative decoding is suggested for general linear block codes with short blocklengths as well [35] and this section basically extends the initialization rules described in the previous section. This extension takes care of the possible intermediate node errors by modifying the LLR values.

For the model detailed in Section 2.2.2, we make use of SP decoding and compare its performance with the optimal one. The aim of the decoding operation is to produce a
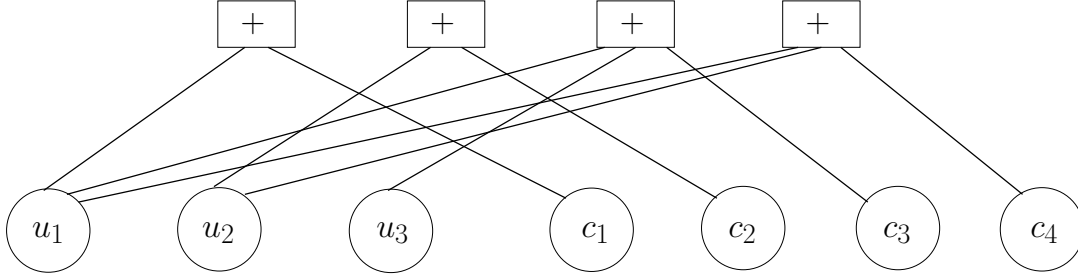
Figure 3.4: Tanner graph for network coded system of (2.5).

posteriori probabilities (APPs) for source symbols $u_1, \ldots, u_k$. To that end, we form a combined codeword $[u_1 \ldots u_k \, c_1 \ldots c_n]$ and consider the parity check (PC) matrix for this codeword, which describes the underlying linear block code structure of the network code. On the Tanner graph, we add a variable node for each source symbol u_i, $i = 1, \ldots, k$ and each coded symbol c_j, $j = 1, \ldots, n$. Afterwards, we add check nodes which reflect the connections between the source and the coded symbols in the way described by the PC matrix. For the NC system of (2.5), we refer to the graph in Fig. 3.4 for SP decoding at node 0. The PC matrix for this system becomes:

$$
\begin{array}{c}
\begin{array}{ccccccc} u_1 & u_2 & u_3 & c_1 & c_2 & c_3 & c_4 \end{array} \\
\begin{array}{l}
\text{PC } 1 \rightarrow \\
\text{PC } 2 \rightarrow \\
\text{PC } 3 \rightarrow \\
\text{PC } 4 \rightarrow
\end{array}
\left[
\begin{array}{ccccccc}
1 & 0 & 0 & 1 & 0 & 0 & 0 \\
0 & 1 & 0 & 0 & 1 & 0 & 0 \\
1 & 0 & 1 & 0 & 0 & 1 & 0 \\
1 & 1 & 0 & 0 & 0 & 0 & 1
\end{array}
\right] = \left[\mathbf{G}^T \vdots \mathbf{I}_n \right],
\end{array} \qquad (3.10)
$$

where $\mathbf{G}^T$ denotes the transpose of $\mathbf{G}$ and $\mathbf{I}_n$ is the $n \times n$ identity matrix. For a regular LDPC decoder, all of the variable nodes are observed through the channel and corresponding to each channel observation an LLR is computed. For our case, the variable nodes u_1, u_2, and u_3 are not observed so the corresponding LLRs are set to 0. The channel LLRs for the remaining nodes ($c_1, \ldots, c_4$) cannot be calculated as in a regular LDPC decoder either, due to the intermediate node errors and by using (2.9)

40

and (2.12), the channel LLR of c_j is:

$$
\begin{aligned}
\text{LLR}(c_j) &= \ln \frac{p(y_j|c_j=0)}{p(y_j|c_j=1)} \\
&= \ln \frac{(1-p_{e_j})p(y_j|\hat{c}_j=0) + p_{e_j}p(y_j|\hat{c}_j=1)}{(1-p_{e_j})p(y_j|\hat{c}_j=1) + p_{e_j}p(y_j|\hat{c}_j=0)} \\
&= \ln \frac{\exp(\text{LLR}(e_j))\exp(\text{LLR}(\hat{c}_j)) + 1}{\exp(\text{LLR}(e_j)) + \exp(\text{LLR}(\hat{c}_j))},
\end{aligned}
\tag{3.11}
$$

where $\text{LLR}(e_j) \triangleq \ln \frac{1-p_{e_j}}{p_{e_j}}$ and

$$
\text{LLR}(\hat{c}_j) \triangleq \ln \frac{p(y_j|\hat{c}_j=0)}{p(y_j|\hat{c}_j=1)} = \frac{4\mathfrak{Re}\left\{h_j^* y_j\right\}}{N_0},
\tag{3.12}
$$

where h_j^* is the conjugated gain of the channel over which the modulated symbol $s_j = \mu(\hat{c}_j)$ is transmitted by node v_j and we use the fact that w_j is Gaussian distributed (see Section 2.2.2) in obtaining $\text{LLR}(\hat{c}_j)$. Given the channel LLRs, the SP decoder carries on iterations over the Tanner graph to generate the estimated LLRs for the source bits. In each iteration, the messages (LLR values) are passed from the check nodes to the variable nodes and vice versa so that each variable node updates its belief on the value of data bit it represent. This message passing is done in parallel fashion so that all variable nodes output their messages simultaneously as a group and so do the check nodes just as for regular LDPC decoding with parallel implementation. If the number of iterations is fixed, the SP decoder utilized is known to have a complexity order of $O(n)$. In contrast, the optimal decoder has a computational load in the order of $O(2^n)$, which makes the SP decoder a strong alternative for increasing network size and number of transmissions. One may also note that the proposed SP decoder works directly with GF(q), $q > 2$, and constellations other than BPSK. The use of higher order fields and constellations would tremendously increase the complexity of the optimal algorithm and make it impractical, whereas the SP algorithm would still operate with reasonable complexity. The number of iterations and other operational parameters for the SP decoder are given in Section 3.3.3, where we show that performance figures close to that of the optimal one are possible for the network codes investigated herein.

3.3.3 Performance of the Sum-Product Decoding for Network Coded Systems

In this section the performance figures for the SP iterative network decoder described in Section 3.3 are presented in comparison with the optimal detection rule of (2.14), which has an exponential complexity order. The first network coded communication system of interest is given in (3.3). The number of iterations for the SP type decoder is limited to 4 and no early termination is done over parity checks. Here, a minimum of 150 bit errors are collected for each data bit.

In Fig. 3.5, we identify the fact that the SP decoder maintains almost the same BER performance as the optimal decoding rule. The SNR loss due to usage of the SP decoder is less than 0.1 dB for a BER value of 10^{-3} for all data bits. Achieving close-to-optimal performance with a linear complexity order, SP type decoding may serve as an ideal method for the network coded system of (3.3) despite the fact that the corresponding Tanner graph contains cycles. Results demonstrating the good performance of SP decoding were also reported previously in [2, 12, 35] for graphs with cycles. In fact, one may realize that the length of the shortest cycle in the corresponding graph is 6, hence the graph is said to have a girth of 6. In [12] within the context of sparse intersymbol interference (ISI) channels, it is shown that for any graph with girth 6, the performance of the SP algorithm is practically optimal. On the other hand, one may identify that for the family of greedy codes for $k = 3$ users with blocklenghts larger than 6, the girth of the corresponding graph will always be 4. Fortunately, it is also given in [12] that the method of *stretching* on girth-4 graphs yields modified girth-6 graphs on which the SP algorithm evaluates the APPs for the data symbols with negligible performance loss. Further details on the girth profile and degree distribution optimization procedures (like in [7] for a greedy search of LDPC codes and like in [8] for root-check LDPC code design) and design of large blocklength MDS network codes achieving full-diversity under SP decoding [31] are out of scope of this work.

In order to further exemplify the effectiveness of the proposed SP network decoder, we present the performance results for a network with more source nodes carrying out more total number of transmissions. Utilizing the $(10, 5, 4)$ greedy code, we construct a NC system with 5 nodes whose data bits are expected to observe a diversity

Figure 3.5: BER curves for the individual MAP decoder of (2.14) and the SP iterative decoder for $(6, 3, 3)$ greedy NC system

order equal to 4 following a round of communication with 10 transmissions. According to Fig. 3.6, where only the data bits with highest and the lowest coding gains are included in order to ease the interpretation of the results, SP network decoder still preserves its close-to-optimal BER performance if its number of iterations is increased to 10 for this larger network.

3.3.4 Performance of Selective Network Coding (SNC) with Greedy Codes and SP Decoding

The selective network encoding operation defined in Section 2.2.4 is applied in this section on the Sample Network-II of Section 3.2.2. The performance improvement for the selective encoding over the static (using fixed $\mathbf{G}$ with no selection of symbols to be encoded) encoding method is again shown using the SP iterative decoder of Section 3.3. The instantaneous intermediate node error probabilities are compared with average error probabilities (dictated by $\mathbf{G}$) and data of the nodes whose error probabilities are below the corresponding average values (thresholds) are combined
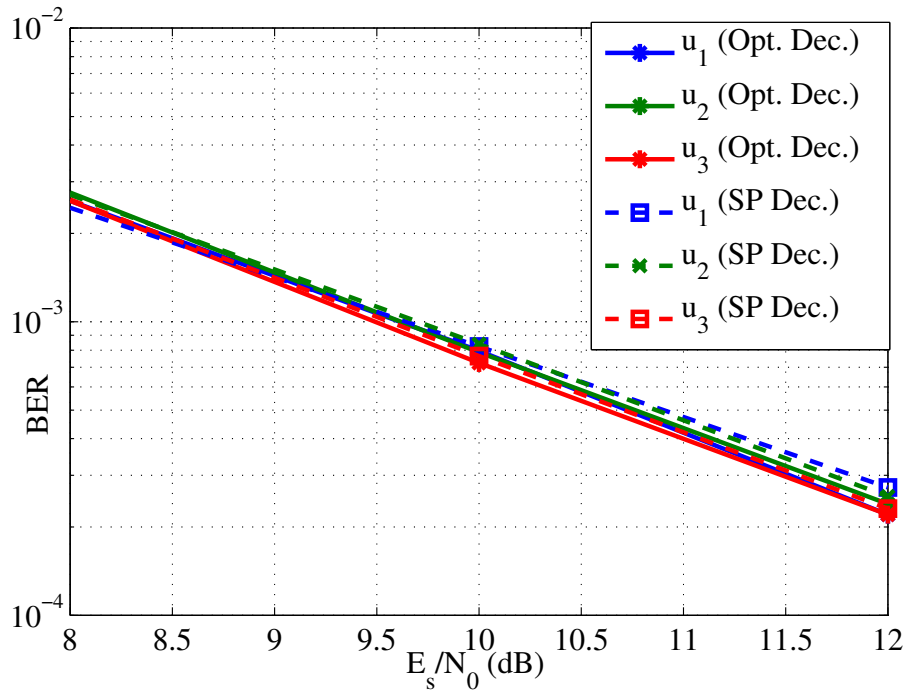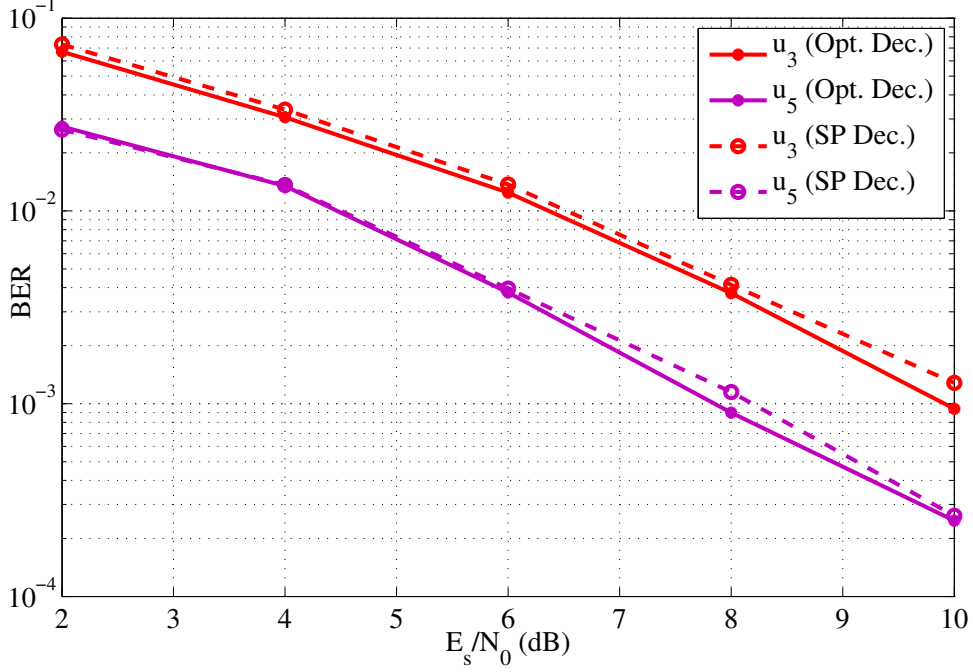
Figure 3.6: BER curves for the individual MAP decoder of (2.14) and the SP iterative decoder for $(10, 5, 4)$ greedy NC system

by the intermediate node. In Fig. 3.7, we observe that SNC offers an SNR improvement of 0.6 dB for BER set to 10^{-3} over the static NC method. Before finalizing this section, we give a simulation result for a network coded system of $k = 4$ source nodes cooperatively transmitting their information bits in $n = 8$ orthogonal time slots. For this purpose we utilize the following greedy code satisfying a diversity order of 4 for each node's bit:

$$\mathbf{G}_3 = \begin{bmatrix} 1 & 0 & 0 & 0 & 1 & 1 & 1 & 0 \\ 0 & 1 & 0 & 0 & 1 & 1 & 0 & 1 \\ 0 & 0 & 1 & 0 & 1 & 0 & 1 & 1 \\ 0 & 0 & 0 & 1 & 0 & 1 & 1 & 1 \end{bmatrix}, \mathbf{v}_3 = \begin{bmatrix} 1\,2\,3\,1\,2\,3\,1 \end{bmatrix}. \quad (3.13)$$

The plotted curves are for the cases: i. Repetition coding scenario with each node transmitting only its own bit twice, ii. Network coded scenario directly dictated by generator matrix and scheduling vector pair given in (3.13), iii. An alternative method which utilizes only the statistics (average BER) as the reliability information in the detection rule instead of instantaneous values to decrease the overhead in the transmis-

44
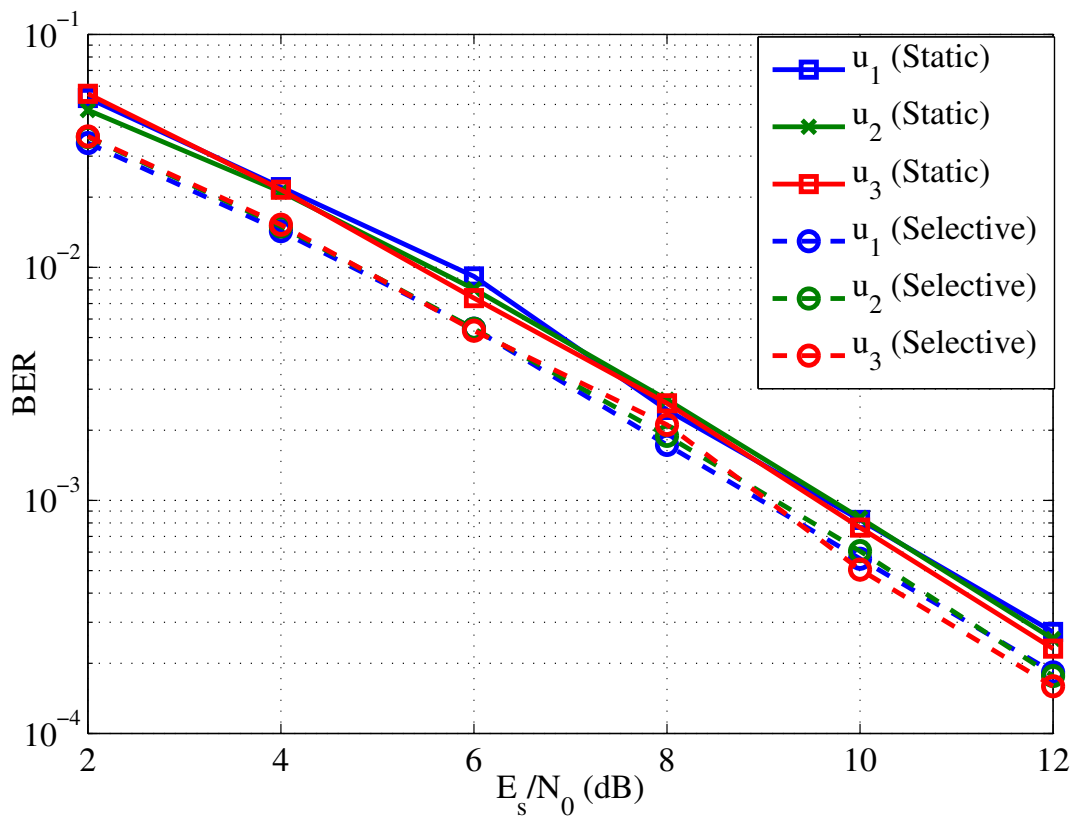
Figure 3.7: Selective and static network encoding BER curves.

sion. iv. SNC utilizing the network coding rules in (3.13) with the constraint on the reliability of each transmission as described in Section 2.2.4. One clearly observes
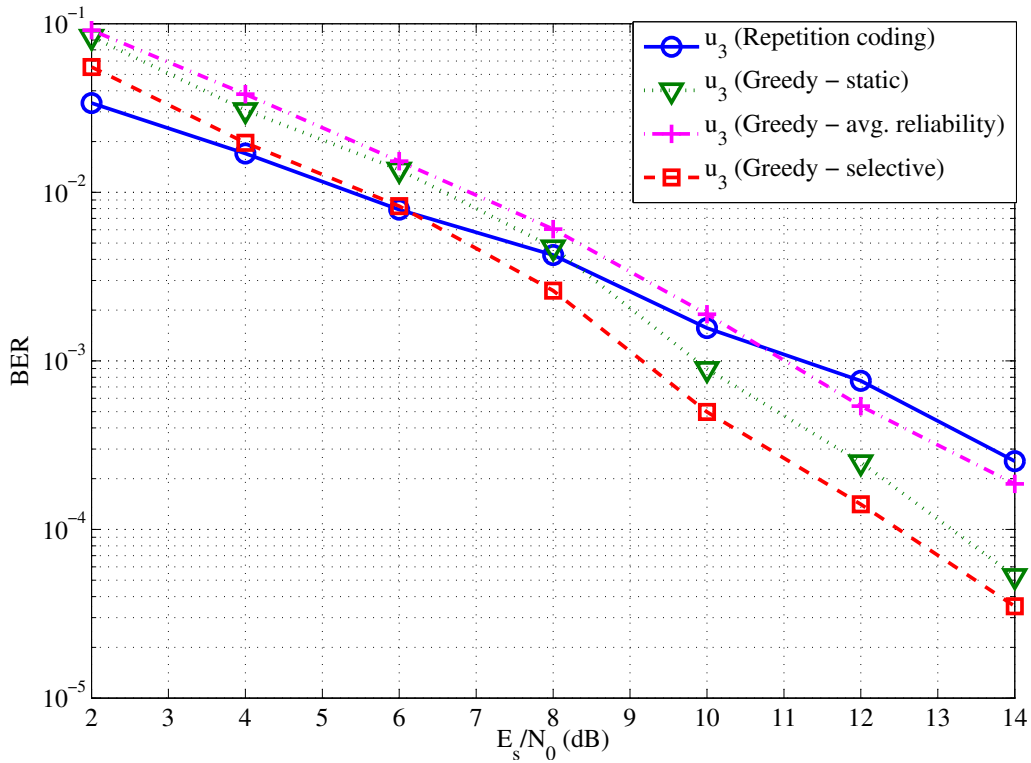
Figure 3.8: Selective and static network encoding BER curves.

that SNC and direct NC satisfy the maximum achievable diversity order, whereas the technique that uses average reliability information results in diversity loss leading to higher SNR requirements for the same BER value. In fact, the gain by resorting to NC under average reliability information with respect to the repetition coding case is limited to only 0.5 dBs. Hence one should prefer to use the instantaneous reliability information from the intermediate nodes in order to fully cover the spatial diversity opportunities offered by the cooperative communications through NC.

3.4 Performance of NC under Slow-Fading Channel Model

All the discussion and the results presented up until this section rely on the assumption that all channel gain coefficients related to the observations at node 0 are independent. Hence a block fading model over time slots is utilized. However, it is also possible under many communication scenarios that the variation of a channel gain coefficient is not rapid enough for such an assumption. Then it is also possible that all transmissions from a selected source node to node 0 observe the same fading condition leading to the degradation in BER performance due to loss in diversity. Therefore, we finalize the numerical results by providing the BER curves of NC and repetition coding under the assumption that within a round of n transmissions, only the transmissions from distinct source nodes observe independent fading, i.e., h_j and h_m are independent if $v_j \neq v_m$ and otherwise $h_j = h_m$. In Fig. 3.9, we plot the BER curves for the Sample Network-II operating under this slower fading assumption. Repetition coding is represented by (3.2) and NC is realized by (3.3). It is seen that repetition coding merely results in a diversity order of 1 for each bit as expected. On the other hand, NC yields an order of 2 via the cooperative diversity obtained due to intermediate nodes transmitting over independent channels. The SNR losses incurred by not utilizing NC are shown to further increase in great amounts in this slower fading scenario.

3.5 Discussion

This section starts with the fundamental performance parameter definition for the NC system and investigates its connection with the separation vector of the underlying linear block code. Then by the support of the family of greedy codes that are readily available for various network sizes with various number of transmissions in order to supply each source node with a desired level of error protection, we provide a theoretic insight into the superiority of NC to the repetition coding method. Moreover, we reach the result that once we fix a desired level of diversity order for each node in a NC system, as we increase the number of nodes the rate advantage of NC gets bigger and converges to the fixed diversity order.

According to the optimal and the suboptimal network decoding rules described in
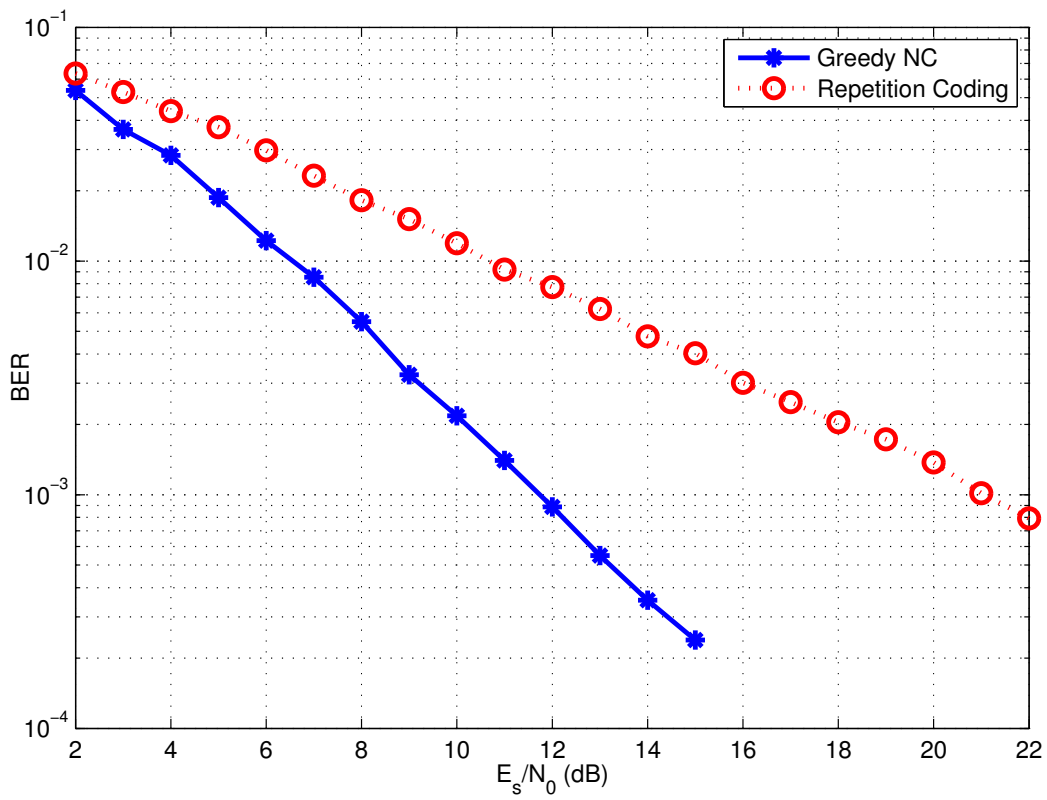
Figure 3.9: BER vs. SNR curves for slow fading channel.

Section 2.2.2, the computational complexity of decoding for the proposed NC system grows exponentially both in the size of the network and in the number of transmissions. In order to decrease this complexity, we propose a novel SP network decoder that operates on a special Tanner graph constructed according to the underlying linear block code. It is also shown through simulations for sample networks in this section that the proposed linear order complexity SP network decoder performs quite close to the optimal rule. Again by operating the proposed SP decoder on two different SNC scenarios we show the improvements obtained, which correspond to SNR gains on the order of 0.5 up to 1 dB.

A final result on the performance improvements owing to the usage of NC idea is presented for slow fading channels, in which the source nodes has only other nodes as means of creating diversity. In this specific scenario, NC is seen to result in huge SNR gains with respect to the repetition of packet with no NC.

CHAPTER 4

EXPECTED BER ANALYSIS FOR THE CANONICAL COOPERATIVE SYSTEM AND NETWORK CODED COOPERATIVE SYSTEM

Our ultimate goal, in this section, is to derive closed form expected end-to-end BER expressions for the network coded cooperative communication system for which the signal model and related detection rules are given in Section 2.2. In order to achieve this goal, we start with some building blocks hidden in the BER analysis of the basic cooperative system of Section 2.1 with C-MRC type detection and equivalent channel assumption at the destination node R. The expected BER expression for this basic system is obtained after generalizing the sampling property introduced in [25] to more than one variables. In addition to this generalization, we present a more complete analysis and an SNR-based characterization of the validity of the sampling property in this section.

4.1 Analysis of the BER Performance of the Basic Cooperative Communication System

The instantaneous end-to-end BER expression for the canonical cooperative system of Section 2.1 is found in [46] as

$$P^b = \left(1 - Q(\sqrt{2\gamma_{SR}})\right) Q\left[\frac{\sqrt{2}(\gamma_{SD} + \gamma_{eq})}{\sqrt{\gamma_{SD} + \gamma_{eq}^2/\gamma_{RD}}}\right]$$

$$+ Q(\sqrt{2\gamma_{SR}})Q\left[\frac{\sqrt{2}(\gamma_{SD} - \gamma_{eq})}{\sqrt{\gamma_{SD} + \gamma_{eq}^2/\gamma_{RD}}}\right]. \tag{4.1}$$

In order to obtain the expected end-to-end BER, one has to evaluate a triple integral for the instantaneous BER function in (4.1) over the related distributions of the random variables γ_{SR}, γ_{SD}, γ_{RD} (here, γ_{eq} is a function of γ_{SR} and γ_{RD}). However, accomplishing this analytically is hard and also the alternative method of resorting to Monte Carlo simulations is time consuming in general. In [46], only the diversity order of the average BER expression is obtained following a series of upper bounding techniques and the result is 2 since two transmissions are made on independent paths in the network and D accounts for possible relaying errors through C-MRC. In the following sections, we develop novel closed form expressions step-by-step for the average BER of this system in which the coding and the diversity gains are identified separately.

4.1.1 Sampling Property of the Q-Function for Generalized Expressions

In this section, firstly, we propose a simple method in order to improve the sampling property of the Q-function that is first presented in [24]. We continue with demonstration of the insufficiency of this sampling property particularly in the low-SNR region. By analysis over the constituent functions involved in a basic expectation integral, we remedy this deficiency and generalize the sampling property for low-SNR region as well. In this way we propose a piecewise approximation to this integral that is close to the simulation results in the low-SNR region as well as the high-SNR region. Finally, the sampling property is further generalized to expectation integrals whose integrand functions involve more than one variables.

4.1.1.1 Basic Problem and its Solution

Assume that the following expectation integral of an instantaneous probability of error function $Q(\sqrt{X})$ is to be evaluated for a random variable X with probability density function (pdf) $f_X(x)$ [24]:

$$I_0 = E_X\left\{Q(\sqrt{X})\right\} = \int_0^\infty Q(\sqrt{x})f_X(x)\mathrm{d}x. \tag{4.2}$$

After the change of variables operation $x \to t^N$, we have the integrand being equal to $Q(\sqrt{t^N})Nt^{N-1}f_X(t^N)$. Here we define the following constituent functions of the integrand.

$$q(t) \triangleq Q(\sqrt{t^N}), \ c(t) \triangleq Nt^{N-1}, \ f(t) \triangleq f_X(t^N). \tag{4.3}$$

In [24], $h(t^N) \triangleq q(t)c(t)$ is defined and claimed to be a unimodal function of t with a critical point satisfying $t_*^N = 2$ and is well-approximated by a Dirac delta as $N \to \infty$. However, that analysis does not show that $h(t^N)$ assumes the value of zero at all other points. On the contrary, when any other finite t^N value is inserted in Eqn. (52) of [24] it is easy to show that $h(t^N)$ assumes infinity. Moreover, the critical point $t_*^N = 2$ is obtained after applying an upper bound on the Q-function. Here, we will take a different approach without any approximations to show that $h(t^N)$ indeed assumes an infinite value only around the point $t = 1$ and converges to 0 everywhere else. In addition, we suggest an alternative way to calculate t_*^N so that the low-SNR agreement with the simulation results is enhanced. We then propose a piecewise sampling method on constituent functions to further improve our technique in the subsequent section.

Let us start with the analysis of the integrand $I(t) \triangleq q(t)c(t)f(t)$ for three distinct regions of t:

$$I_0 = \int_0^{1^-} I(t)\mathrm{d}t + \int_{1^-}^{1^+} I(t)\mathrm{d}t + \int_{1^+}^\infty I(t)\mathrm{d}t. \tag{4.4}$$

It should be emphasized that the value I_0 in (4.4) is independent of N and hence we may investigate the behaviour of $I(t)$ asymptotically (as $N \to \infty$). In this work, we take $f(t) = \frac{1}{SNR}e^{-\frac{t^N}{SNR}}$ due to the Rayleigh fading model assumed for the channels in the network. However, the following steps can be generalized to other pdfs easily.

Initially, for the $0 < t < 1$ region, we reach the following asymptotic result for the convergence of the integrand function:

$$\lim_{N\to\infty} I(t)\Big|_{0<t<1} = \left(\lim_{N\to\infty} q(t)\right)\left(\lim_{N\to\infty} c(t)\right)\left(\lim_{N\to\infty} f(t)\right)$$

$$= \left(\frac{1}{2}\right)\left(\lim_{N\to\infty} \frac{1}{\ln t(-t^{1-N})}\right)\left(\frac{1}{SNR}\right)$$

$$= 0, \tag{4.5}$$

where the L'Hôpital rule is applied for $\lim_{N\to\infty} c(t)$ term and the product law for limits is utilized. As a result, the first integral in (4.4) evaluates to 0 asymptotically. Next, for the $t > 1$ region, we obtain

$$\lim_{N\to\infty} I(t)\Big|_{t>1} = \left(\lim_{N\to\infty} q(t)\right)\left(\lim_{N\to\infty} c(t)f(t)\right)$$

$$= (0)\left(\lim_{N\to\infty} \frac{Nt^{N-1}}{\exp\left(\frac{t^N}{SNR}\right)}\right)\left(\frac{1}{SNR}\right)$$

$$= (0)\left(\lim_{N\to\infty} \frac{t^{N-1} + N(\ln t)t^{N-1}}{\frac{\ln t}{SNR}t^N \exp\left(\frac{t^N}{SNR}\right)}\right)$$

$$= (0)\left(\lim_{N\to\infty} \frac{\ln t}{\left(\frac{\ln t}{SNR}\right)^2 t^N \exp\left(\frac{t^N}{SNR}\right)}\right)$$

$$= 0 \tag{4.6}$$

following the application of the L'Hôpital rule twice. Hence, in the asymptotic sense, the third integral in (4.4) does not contribute to the result either. Therefore, we conclude that

$$I_0 = \int_{1^-}^{1^+} \lim_{N\to\infty} I(t)\mathrm{d}t, \tag{4.7}$$

which shows us that the integrand $I(t)$ may be well-approximated by a Dirac delta generalized function at $t = 1$ for $N \to \infty$. Moreover, it can be shown that this Dirac delta approximation also holds for the function $h(t^N) \triangleq q(t)c(t)$ by following the arguments utilized in reaching (4.5) and (4.6). As an example, in Fig. 4.1, we plot the

54

function $h(t^N)$ around $t = 1$ for $N = 100$ and $N = 1000$. Clearly, this function is better and better approximated by a Dirac delta as we increase N. On the other hand, it is quite easy to reach the result that $g(t^N) \triangleq f(t)c(t)$ is also non-zero only for $t = 1$ as $N \to \infty$ and can be approximated by another Dirac delta. Therefore, we should select one of the functions $h(t^N)$ and $g(t^N)$ to be approximated by a Dirac delta according to their behaviour at points other than $t = 0$. This means, it is important to characterize these functions in the regions $t < 1$ and $t > 1$ in order to select the one with faster decay rate to zero. Next, we are going to identify two average SNR values above and below which $h(t^N)$ and $g(t^N)$ can be safely approximated by a Dirac delta respectively in Section 4.1.1.2.
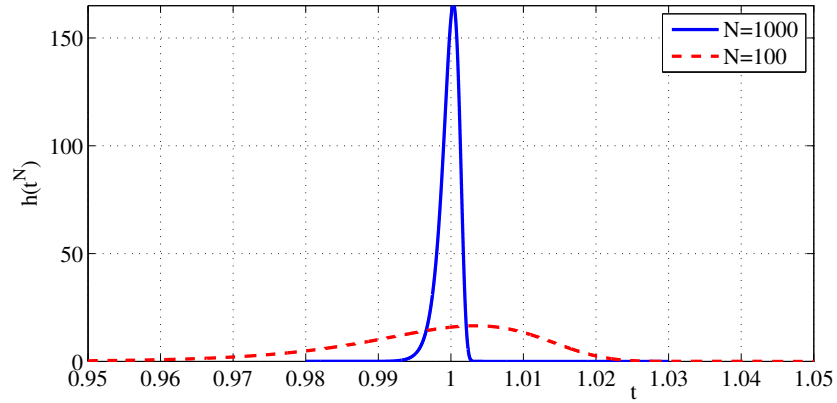
Figure 4.1: Convergence of $h(t^N)$, $N = 100$ and 1000

4.1.1.2 Rates of Convergence for Constituent Functions

In order to approximate the basic integral of (4.2) by using the sampling property, we need to obtain two essential parameters of the Dirac delta generalized function, which is an approximation to one of the constituent functions $h(t^N)$ or $g(t^N)$. The first parameter is the location of Dirac delta, t_*^N. The asymptotic (as $N \to \infty$) critical point of the function of interest yields this parameter and the critical point can be either found analytically or by solving a simple unconstrained optimization problem. The

other parameter is the weight of the function c and is analytically obtained for both of the constituent functions by integrating the related function from 0 to ∞. However, another important issue is to pick the sampling function as one of $h(t^N)$ or $g(t^N)$ according to their asymptotic convergence rates to the function that is approximated by a Dirac delta at $t = 1$.

We start with comparing the convergence rates of $h(t^N)$ and $g(t^N)$ for $0 < t < 1$ and $t > 1$, separately. Firstly, consider the region $0 < t < 1$. For this region, both $q(t)$ and $f(t)$ converge to nonzero constants in the limit. On the other hand, the function $c(t) = Nt^{N-1}$ converges to 0, which means that for large N, $h(t^N)$ and $g(t^N)$ converge to 0 with the same rate. Hence we focus on the other region: $t > 1$. In this region, we compare $h(t^N)$ and $g(t^N)$ for distinct average SNR regions. Let us start with the Chernoff upper bound on the Q-function:

$$q(t)\Big|_{t^N=x} = Q(\sqrt{x}) \leq \frac{1}{2}\exp\left(-\frac{x}{2}\right). \tag{4.8}$$

In addition, for $t > 1$ and $SNR \geq 2$ it is easily shown that

$$f(t)\Big|_{t^N=x} = \frac{\exp\left(\frac{-x}{SNR}\right)}{SNR} \geq \frac{1}{2}\exp\left(-\frac{x}{2}\right). \tag{4.9}$$

Combining (4.8) and (4.9) for $t > 1$ and $SNR \geq 2$ (in dB scale roughly for values larger than 3 dB) we get

$$q(t)\Big|_{t^N=x} \leq f(t)\Big|_{t^N=x}. \tag{4.10}$$

Using (4.10) we reach the result that for $SNR > 2$, $h(t^N)$ (including the Q-function) is better represented by a Dirac delta with respect to $g(t^N)$ (including the exponential pdf). This is in accordance with the previous results in [25] that for high SNR, Q-function may be approximated by a Dirac delta well. On the other hand, for $t > 1$ and $SNR < 1/3$ (roughly less than -5 dB), one can show that

$$q(t)\Big|_{t^N=x} = Q(\sqrt{x}) \geq \frac{1}{\frac{1}{3}}\exp\left(-\frac{x}{\frac{1}{3}}\right) \geq \frac{\exp\left(\frac{-x}{SNR}\right)}{SNR} = f(t)\Big|_{t^N=x}. \tag{4.11}$$

Consequently, for lower SNR values, $g(t^N)$ is more suitable for the sampling function definition. Firstly, the position of the Dirac delta that approximates $g(t^N)$ can be

obtained by finding the critical point t_g^N. We equate the first derivative of $g(t^N)$ with respect to t to 0:

$$\frac{\mathrm{d}}{\mathrm{d}t} g(t^N) \bigg|_{t^N = t_g^N} = 0, \qquad (4.12)$$

whose solution is

$$t_g^N = \frac{N-1}{N} SNR. \qquad (4.13)$$

Eqn. (4.13) gives us the asymptotic critical point $t_*^N = \lim_{N \to \infty} t_g^N = SNR$. Second, the weight of the corresponding Dirac delta is found as 1 due to the normalization property of the pdf. Hence for $SNR < 1/3$, we may use the approximation $I_0 \approx \int_0^\infty Q(\sqrt{x})\delta(x - SNR)\mathrm{d}x = Q\left(\sqrt{SNR}\right)$. For $SNR > 2$, we write $I_0 \approx \int_0^\infty c\delta(x - t_*^N) f_X(x)\mathrm{d}x = \frac{c}{SNR} \exp\left(-\frac{t_*^N}{SNR}\right)$, where the impulse weight is found using the alternative definition of Q-function as $c = \int_0^\infty h(t^N)\mathrm{d}t = \int_0^\infty Q(\sqrt{x})\mathrm{d}x = \frac{1}{2}$ analytically.
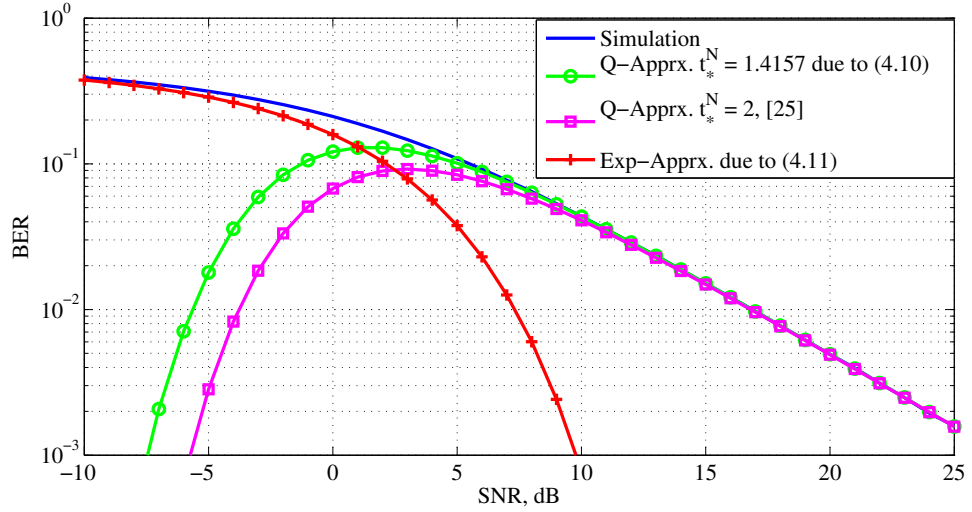

Figure 4.2: Approximating the integral I_0 using various methods

We propose a simple alternative to the method in [24] to evaluate the location of the impulse which approximates $h(t^N)$. For a sufficiently large value of N, we pose finding the critical point as an unconstrained optimization problem and employ numerical

57

search to find the solution. In a narrow neighbourhood of $t = 1$, we search for the critical point of $h(t^N)$, as an example by using the Optimization Toolbox function *fminsearch()* of MATLAB. In MATLAB, we find $t_*^N = 1.4157$ just after 4 iteration steps, whereas in [24] $t_*^N = 2$ was considered. The error rate curves from approximations as well as simulations are given in Fig. 4.2. According to Fig. 4.2, the methods approximating $h(t^N)$ as a Dirac delta (one proposed in [24] with square markers, and the one we propose with circular markers) are quite consistent for high SNR values. However, the method using unconstrained optimization for searching the impulse location is the better one with close approximation for $SNR > 3$dB as detailed in equation (4.10). For low SNR values, on the other hand, only the method selecting $g(t^N)$ as the sampling function (plus shaped markers) is close to the simulation result. This shows us that for a close approximation of the integral I_0 over the whole SNR region, we need to use a piecewise function. In the following sections, with integrands of more than one variables, we are going to use only the sampling property for the Q-function since we are mostly interested in the high SNR regime.

4.1.1.3 Two-Variable Sampling Property

In this section we base our discussion on the following integral involving two variables in the integrand.

$$I_1 = \int_0^\infty \int_0^\infty Q(\sqrt{a_1 x + a_2 y}) f_X(x) f_Y(y) \mathrm{d}x \mathrm{d}y, \qquad (4.14)$$

where a_1 and a_2 are positive constants. The form of the expectation integral given in (4.14) is frequently observed for receivers collecting observations on two independent channels and combining these received signals according to MRC operation. In the scenario of basic relayed communication, similar expectation integrals are also encountered [24–26], however no higher dimensional generalization for sampling property has been made in the literature as far as we know. In [25], a two-dimensional integrand is approximated by two single variable integrands resulting in coding gain offsets in the final expressions.

Similar to the single dimension analysis, we define a new function following the change of variables operation $h(t^N, u^N) \triangleq Q(\sqrt{a_1 t^N + a_2 u^N}) N^2 t^{N-1} u^{N-1}$ based

on the Q-function. We simply pick $h(t^N, u^N)$ as the sampling function, since it is shown to perform well in the high-SNR region in Section 4.1.1.2. Here, it is easy to generalize the asymptotic analysis for $h(t^N, u^N)$ with $N \to \infty$ to show that it is well-approximated by a two-dimensional Dirac delta at $(t, u) = (1, 1)$. This is further exemplified in Fig. 4.3 for $N = 1000$ and $a_1 = a_2 = 2$.
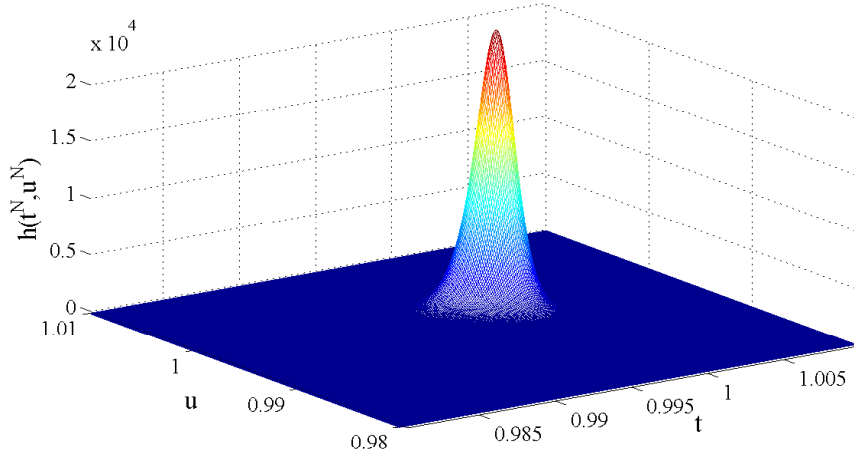
Figure 4.3: Function $h(t^N, u^N)$ for $N = 1000$ and $a_1 = a_2 = 2$

Through the unconstrained optimization solution, the critical point of $h(t^N, u^N)$ is computed as $(t_*^N, u_*^N) = (0.8197, 0.8197)$ and the weight of the Dirac delta is analytically found as $c = \int_0^\infty \int_0^\infty Q(\sqrt{a_1 x + a_2 y}) \mathrm{d}x \mathrm{d}y = \frac{3}{4a_1 a_2}$. As an example for $a_1 = a_2 = 2$, the approximation for I_1 is

$$I_1 \approx \frac{3}{16 SNR^2} \exp\left(-\frac{2(0.8197)}{SNR}\right). \tag{4.15}$$

The result in (4.15) is in accordance with the average BER analysis result of the MRC technique applied on two parallel branches [17] and is also very close to the simulation result for mid- to high SNR values as given in Fig. 4.4.

59

4.1.1.4 Sampling in Single Dimension for Functions of Two Variables

Unfortunately, not every integrand function can be simply approximated with a two dimensional Dirac delta as in Section 4.1.1.3. As an example, the instantaneous BER function $Q(\sqrt{2\min\{x,y\}})$ can be investigated. This type of instantaneous BER function prevalently occurs in relayed communication system performance analysis, particularly in the works that approximate the $S-R$ and $R-D$ links with a single link possessing the minimum one of the instantaneous SNR values of these links [16, 46, 54]. Therefore, the average BER function for these systems is also important and requires the evaluation of the following integral:

$$
\begin{aligned}
I_2 &= E_{X,Y}\left\{Q(\sqrt{2\min\{x,y\}})\right\} \\
&= \int_0^\infty \int_0^\infty Q(\sqrt{2\min\{x,y\}})f_X(x)f_Y(y)\mathrm{d}x\mathrm{d}y.
\end{aligned}
\tag{4.16}
$$

Here, it can be shown that the constituent function related to the Q-function within the integrand is $h(t^N, u^N) \triangleq Q(\sqrt{2\min\{t^N, u^N\}})N^2 t^{N-1} u^{N-1}$ following the corresponding change of variables operation. One observes that $h(t^N, u^N)$ diverges also at points other than $(t, u) = (1, 1)$ unlike the constituent function of the previous section. However, it is still possible to analyze this function using the fact that $Q(\sqrt{2\min\{x,y\}}) \le Q(\sqrt{2x}) + Q(\sqrt{2y})$ and the sampling property for single variable functions given in Section 4.1.1.1. Then we can reach the following approximation for this expectation integral, which is shown to perfectly fit the simulation result in Fig. 4.4.

$$
\begin{aligned}
I_2 &= \int_0^\infty \int_0^\infty Q(\sqrt{2\min\{x,y\}})f_X(x)f_Y(y)\mathrm{d}x\mathrm{d}y \\
&\le \int_0^\infty \int_0^\infty Q(\sqrt{2x})f_X(x)\mathrm{d}x + \int_0^\infty \int_0^\infty Q(\sqrt{2y})f_Y(y)\mathrm{d}y \\
&\approx \frac{1}{2SNR}\exp\left(-\frac{0.7079}{SNR}\right).
\end{aligned}
\tag{4.17}
$$

4.1.2 BER analysis for the Canonical Cooperative Model

The end-to-end instantaneous BER function in (4.1) can be written as the sum of two terms: $P^b = P_1 + P_2$. Let us start with P_1:

$$P_1 = \left(1 - Q(\sqrt{2\gamma_{SR}})\right) Q \left[\frac{\sqrt{2}(\gamma_{SD} + \gamma_{eq})}{\sqrt{\gamma_{SD} + \gamma_{eq}^2/\gamma_{RD}}} \right], \qquad (4.18)$$

which is a function of three variables, γ_{SR}, γ_{RD}, and γ_{SD}. Similar to the analysis in Section 4.1.1.4, function P_1 can not be approximated with a Dirac delta directly, due to the variable γ_{eq} defined over the instantaneous SNR values of the two-hop link, γ_{RD} and γ_{SD}. Therefore, we define two terms that are asymptotic in γ_{RD} and γ_{SD} following the approach in Eqn. (42) of [25]

$$P_1^{\gamma_{RD}} \triangleq \lim_{\gamma_{RD} \to \infty} P_1 = \left(1 - Q(\sqrt{2\gamma_{SR}})\right) Q \left[\frac{\sqrt{2}(\gamma_{SD} + \gamma_{SR})}{\sqrt{\gamma_{SD}}} \right]$$

$$P_1^{\gamma_{SR}} \triangleq \lim_{\gamma_{SR} \to \infty} P_1 = Q \left[\sqrt{2(\gamma_{SD} + \gamma_{RD})} \right] \qquad (4.19)$$

to approximate P_1 with the sum of these two terms, $P_1 \approx P_1^{\gamma_{RD}} + P_1^{\gamma_{SR}}$. In this way, P_1 is now the sum of two functions both of which have two arguments and are suitable for an approximation with impulse functions. It should be noted that in the approach utilized in Section 4.1.1.4, $Q(\sqrt{2x})$ and $Q(\sqrt{2y})$ are also asymptotic terms. Using the result of Section 4.1.1.3, taking $\sigma_{SD}^2 = \sigma_{SR}^2 = \sigma_{RD}^2 = 1$ and average SNR as $\bar{\gamma}$, approximate expectation of P_1 is evaluated to be

$$I_3 \approx \int_0^\infty \int_0^\infty P_1^{\gamma_{RD}} f_{\gamma_{SR}}(\gamma_{SR}) f_{\gamma_{SD}}(\gamma_{SD}) \mathrm{d}\gamma_{SR} \mathrm{d}\gamma_{SD}$$

$$+ \int_0^\infty \int_0^\infty P_1^{\gamma_{SR}} f_{\gamma_{RD}}(\gamma_{RD}) f_{\gamma_{SD}}(\gamma_{SD}) \mathrm{d}\gamma_{RD} \mathrm{d}\gamma_{SD}$$

$$\approx \frac{1}{16\bar{\gamma}^2} \exp\left(-\frac{1.3049}{\bar{\gamma}}\right) + \frac{3}{16\bar{\gamma}^2} \exp\left(-\frac{2(0.8197)}{\bar{\gamma}}\right). \qquad (4.20)$$

Defining similar asymptotic terms for P_2, we reach $P_2^{\gamma_{RD}} = Q(\sqrt{2\gamma_{SR}})Q\left[\frac{\sqrt{2}(\gamma_{SD} - \gamma_{SR})}{\sqrt{\gamma_{SD}}}\right]$ and $P_2^{\gamma_{SR}} = 0$. Therefore, the following integral approximation can be found for expectation of P_2 by making use of 2D sampling property once more.

$$I_4 \approx \int_0^\infty \int_0^\infty P_2^{\gamma_{RD}} f_{\gamma_{SR}}(\gamma_{SR}) f_{\gamma_{SD}}(\gamma_{SD}) \mathrm{d}\gamma_{SR} \mathrm{d}\gamma_{SD}$$

$$\approx \frac{1}{4\bar{\gamma}^2} \exp\left(-\frac{1.7564 + 1.3737}{\bar{\gamma}}\right). \tag{4.21}$$

Finally, summing the results of (4.20) and (4.21) we obtain and plot the approximate expectation of P^b as $I_3 + I_4$ in Fig. 4.4 together with the simulation result. It is seen that the analysis proposed in this work yields an extremely good approximation to the end-to-end average BER of the canonical cooperative communication system by giving the closed form expression as a product of the coding and diversity gain terms. We initially observe that the $\exp\left(\frac{-c}{SNR}\right)$ terms will vanish as SNR tends to infinity, where the diversity order and the coding gain are defined. Hence, firstly, the diversity gain is taken as the exponent of the $\frac{1}{\bar{\gamma}}$ terms from (4.20) and (4.21) and is 2 as found in [46]. Then the coding gain is calculated as the sum of the constants multiplying the terms that are functions of SNR and is simply $1/2$.
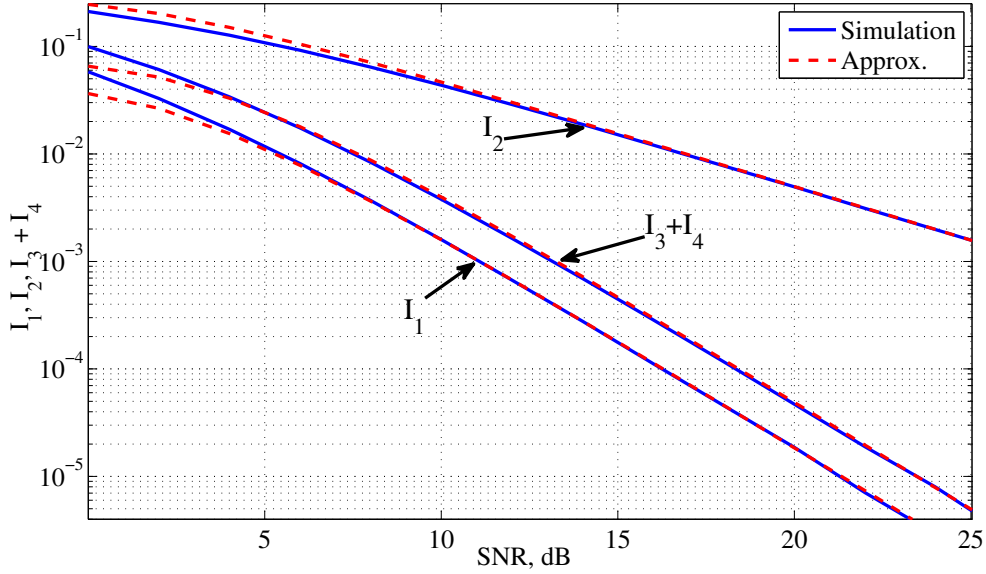
Figure 4.4: Approximating the integrals I_1, I_2, and $I_3 + I_4$

4.2 Analysis of the BER Performance of Wireless Network Coding

The procedure followed in Section 4.1.2 for the analysis of canonical cooperative communication system is extended for the network coded system in this section. The analysis is also based on the receiver structure which utilizes the equivalent channel approximation for the two-hop links carrying the network coded bits. The difference from Section 4.1.2 is that now the receiver should also decode the network code for detecting k source bits rather than detecting a single source's bit by applying simple MRC method on its weighted observation signals. We start with the network coded system description.

4.2.1 A Sample Network Coded System

The network coded communication system analyzed in this section is a sample scenario selected according to the model which is detailed in [6]. In [6], source nodes transmit in orthogonal time slots and each source node serves potentially as a relay to the other source nodes.

Figure 4.5: A sample network coded wireless communication scenario.

The specified network coding scenario is depicted in Fig. 4.5. In the sample network, $k = 3$ source nodes are allowed to transmit to a separate destination, node 0, following a time-division access method with a round of communication that comprises $n =$

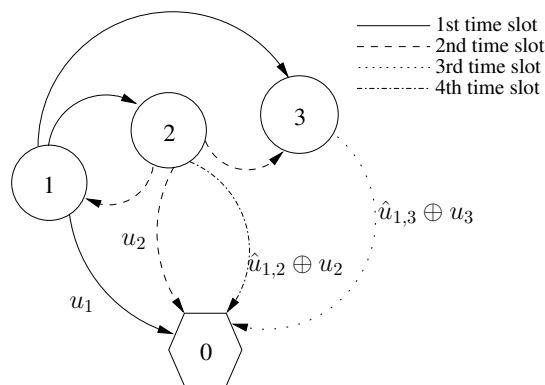4 time slots. The source nodes 1, 2, and 3 aim to transmit their data symbols u_1, u_2, and u_3 respectively. In this work, we assume u_i to be binary for the sake of a simple system description and performance analysis, although all of the following arguments can be generalized for larger alphabets. The network coding rules followed are prescribed by the generator matrix $\mathbf{G}$ and the scheduling of the nodes to use the channel is given in the transmitting node vector $\mathbf{v}$:

$$\mathbf{G} = \begin{bmatrix} 1 & 0 & 1 & 1 \\ 0 & 1 & 0 & 1 \\ 0 & 0 & 1 & 0 \end{bmatrix}, \mathbf{v} = [1\,2\,3\,2]. \tag{4.22}$$

We assume that all the channels associated to the links drawn in Fig. 4.5 follow independent Rayleigh block fading (constant during a time slot) and the channel state information is only available to the receiving end of each link without any feedback in the network. In addition, as described in [6], the intermediate nodes help mitigate the problem of error propagation in the subsequent hops. As an example, the transmission of network coded bit $\hat{u}_{1,3} \oplus u_3$ is based on a possibly erroneous detection at the intermediate node 3. Therefore the intermediate nodes are assumed to append the probability of error in their network coding operation to the transmitted packets so that the destination node 0 can take the possible detection errors into consideration. Under these assumptions, node 0, which is responsible for decoding the source nodes' data, collects the following $n = 4$ observations

$$
\begin{aligned}
y_1 &= h_1 \mu(u_1) + n_1, \\
y_2 &= h_2 \mu(u_2) + n_2, \\
y_3 &= h_3 \mu(u_1 \oplus e_3 \oplus u_3) + n_3, \\
y_4 &= h_4 \mu(u_1 \oplus e_4 \oplus u_2) + n_4, \tag{4.23}
\end{aligned}
$$

where h_j, $j = 1, \ldots, 4$, denotes the independent channel gain coefficient for the jth slot and is assumed to follow $CN(0,1)$. Also n_j, $j = 1, \ldots, 4$, denotes the ZMCSCG noise signal term and is assumed to be independent from all other noise terms, channel coefficients, and data bits. Each noise term has a variance of N_0. We use the mapping $\mu(u_i) = \sqrt{E}(1 - 2u_i)$ with BPSK modulation. We further define

the average SNR as $\bar{\gamma} = \frac{E}{N_0}$ and hence the instantaneous SNR corresponding to each time slot as $\gamma_j = \bar{\gamma}|h_j|^2$, $j = 1, \ldots, 4$. Moreover, e_j is the binary error term for the network coding operation in the jth slot. As a demonstration, if node 3 has detected u_1 bit correctly in the first slot, we have $e_3 = 0$ and $e_3 = 1$ otherwise. Clearly, for the first two slots in which no network coding is utilized we should have $e_1 = e_2 = 0$ deterministically.

4.2.2 BER Analysis for the Sample System Using Equivalent Channel Approach

Let us start investigating (4.23) with emphasis on the observations in the third and the fourth time slots in which network coded cooperation is utilized. For these observations, in order to simplify both the design of the receiver and the analysis, we define the equivalent instantaneous SNR values $\gamma_{eq3} = \bar{\gamma}|h_{eq3}|^2$ and $\gamma_{eq4} = \bar{\gamma}|h_{eq4}|^2$ as done in Section 2.1.

$$\gamma_{eq3} = \frac{\left\{ Q^{-1} \left[p_{e3} \left(1 - Q\left(\sqrt{2\gamma_3}\right)\right) + (1 - p_{e3}) Q\left(\sqrt{2\gamma_3}\right) \right] \right\}^2}{2}, \qquad (4.24)$$

where p_{e3} denotes the probability that node 3 detects u_1 in error (hence forwards an erroneous network coded bit) and with BPSK modulation it is found as $p_{e3} = Q\left(\sqrt{2\gamma_{1\to3}}\right)$ with given instantaneous SNR value $\gamma_{1\to3}$ for the link from node 1 to 3 in the first time slot. Similarly, another equivalent gain γ_{eq4} is defined and the weighted observation signal vector at the receiver $\mathbf{z} = [z_1\ z_2\ z_3\ z_4]$ is found according to

$$
\begin{aligned}
z_1 &= w_1 y_1 = h_1^* y_1 = |h_1|^2 \mu(u_1) + h_1^* n_1, \\
z_2 &= w_2 y_2 = h_2^* y_2, \\
z_3 &= w_3 y_3 = \frac{\gamma_{eq3}}{\gamma_3} h_3^* y_3, \\
z_4 &= w_4 y_4 = \frac{\gamma_{eq4}}{\gamma_4} h_4^* y_4.
\end{aligned}
\qquad (4.25)
$$

In (4.25), the weights for the first two observations are exactly the same as those of the MRC technique, since both of these are direct transmissions with no network coding. Given the equivalent channel outputs in (4.25), one can modify both the joint and the

individual detection rules given in Section 2.2.2 for detection of data vector $\mathbf{u}$. The individual detection rule for u_1 is

$$\hat{\hat{u}}_1 = \arg\max_{u_1 \in \{0,1\}} \sum_{u_2, u_3 \in \{0,1\}} p(\mathbf{z} \mid \mathbf{u}), \qquad (4.26)$$

while the joint detection rule for $\mathbf{u}$ is found as

$$\hat{\hat{\mathbf{u}}} = \arg\max_{\mathbf{u} \in \{0,1\}^k} p(\mathbf{z} \mid \mathbf{u}). \qquad (4.27)$$

Although both of these detectors are very close in terms of BER performance to the optimal detector of (2.14) as to be shown in Section 4.3, the joint detector in (4.27) is much simpler to analyze (and also to implement) due to absence of the summation operation over all possible data vectors. As a consequence, we aim to reach an expected BER expression for the joint detector using the sampling property of the Q-function. This expression is going to be an upper bound for the optimal detector in (2.14).

We start the analysis of the detector in (4.27) by identifying the conditional probability distributions (for given respective channel coefficients) of the weighted observations. Without loss of generality, we take $N_0 = 1$ for the remaining part of the paper in order to simplify the derivation. The transmissions in the first two time slots are direct, hence the distributions of weighted observations are relatively simple. As an example, by further conditioning the observations on the input data vector pattern $u_1 = u_2 = u_3 = 0$, one finds

$$(z_j | u_1 = u_2 = u_3 = 0) \sim CN\left(\gamma_j, \gamma_j\right), \ j \in \{1, 2\}, \qquad (4.28)$$

where the complex Gaussian distribution of the noise signal is used. These distributions are also used in the detector that makes use of the equivalent channel approach. On the other hand, for the slots making use of network coding with possible propagation of binary errors, we obtain the following conditional distribution for the given data and error pattern $u_1 = u_2 = u_3 = e_3 = e_4 = 0$:

$$(z_j | u_1 = u_2 = u_3 = e_j = 0) \sim CN\left(\gamma_{eqj}, \frac{\gamma_{eqj}^2}{\gamma_j}\right), \ j \in \{3, 4\}. \qquad (4.29)$$

However, the equivalent channel detector uses the following distributions (without any consideration on the relay error variables e_j) in the construction of the detection rules

$$(z_j|u_1 = u_2 = u_3 = 0) \sim CN\left(\gamma_{eqj}, \gamma_{eqj}\right), \; j \in \{3, 4\}. \qquad (4.30)$$

since it assumes the network coded data signals are being transmitted over the equivalent channel with no relay error but decreased instantaneous SNR, γ_{eqj}. As a result, in the analysis of the conditional BER for $u_1 = u_2 = u_3 = e_3 = e_4 = 0$, we derive the detection rules according to (4.30), whereas the probability of an error for a detection rule is calculated using (4.29) for the time slots 3 and 4. Similar distributions can also be found for the condition $e_j = 1$.

Due to linearity of the block code used for constructing the network code in the system, one can assume all-zero data vector transmission, $u_1 = u_2 = u_3 = 0$, and find the probability of error for a given data symbol. As an example, for u_1 we have the following upper bound for end-to-end bit error probability:

$$
\begin{aligned}
P(\hat{\hat{u}}_1 \neq u_1) &= \sum_{u_2, u_3} P(\hat{\hat{\mathbf{u}}} = [1 \; u_2 \; u_3] \mid \mathbf{u} = [0 \; 0 \; 0]) \\
&\leq \sum_{u_2, u_3} P(p_{eq}(\mathbf{z} \mid [0 \; 0 \; 0]) < p_{eq}(\mathbf{z} \mid [1 \; u_2 \; u_3])), \qquad (4.31)
\end{aligned}
$$

where we make use of the union bound in the inequality. In (4.31) p_{eq} denotes the pdf utilized by the detector and is found for any data vector $\mathbf{u}$ in a similar fashion to (4.30):

$$p_{eq}(\mathbf{z} \mid \mathbf{u})) = \prod_{j=1}^{4} \frac{\exp\left(-\frac{\left|z_j - (-1)^{\mathbf{u}\mathbf{g}_j} \gamma_{eqj}\right|^2}{\gamma_{eqj}}\right)}{\pi \gamma_{eqj}}, \qquad (4.32)$$

where $\mathbf{g}_j$ is the jth column of the network code generator matrix $\mathbf{G}$ and due to the fact that no intermediate errors occur in direct transmissions $\gamma_{eqj} = \gamma_j$ for $j = 1, 2$. We then condition $P(p_{eq}(\mathbf{z} \mid [0 \; 0 \; 0]) < p_{eq}(\mathbf{z} \mid [1 \; u_2 \; u_3]))$ on the intermediate node error vectors. For the condition $e_3 = e_4 = 0$, by using (4.32), we obtain

$$P\left(p_{eq}(\mathbf{z} \mid [0\ 0\ 0]) < p_{eq}(\mathbf{z} \mid [1\ u_2\ u_3]) \Big| e_3 = e_4 = 0\right) =$$
$$P\left(\prod_{j=1}^{4} \exp\left(-\frac{|z_j - \gamma_{eqj}|^2}{\gamma_{eqj}}\right) < \prod_{j=1}^{4} \exp\left(-\frac{|z_j - (-1)^{([1\ u_2\ u_3]g_j)}\gamma_{eqj}|^2}{\gamma_{eqj}}\right)\right)$$

$$(4.33)$$

As an example, for the erroneously detected vector $\hat{\mathbf{u}} = [1\ 0\ 0]$, we rewrite (4.33) as

$$P\left(p_{eq}(\mathbf{z} \mid [0\ 0\ 0]) < p_{eq}(\mathbf{z} \mid [1\ 0\ 0]) \Big| e_3 = e_4 = 0\right) = P\left(RE\left\{z_1 + z_3 + z_4\right\} < 0\right)$$
$$= Q\left(\frac{\sqrt{2}\left(\gamma_1 + \gamma_{eq3} + \gamma_{eq4}\right)}{\sqrt{\gamma_1 + \frac{\gamma_{eq3}^2}{\gamma_3} + \frac{\gamma_{eq4}^2}{\gamma_4}}}\right),$$

$$(4.34)$$

where we used (4.28) and (4.29) in the last identity. In the next step of derivation for instantaneous BER expression, we sum up the conditional probability terms for all data vectors in error to reach the conditional version of (4.31) with $e_3 = e_4 = 0$ as

$$P(\hat{\hat{u}}_1 \neq u_1 \Big| e_3 = e_4 = 0) \leq Q\left(\frac{\sqrt{2}\left(\gamma_1 + \gamma_{eq3} + \gamma_{eq4}\right)}{\sqrt{\gamma_1 + \frac{\gamma_{eq3}^2}{\gamma_3} + \frac{\gamma_{eq4}^2}{\gamma_4}}}\right) + Q\left(\frac{\sqrt{2}\left(\gamma_1 + \gamma_{eq4}\right)}{\sqrt{\gamma_1 + \frac{\gamma_{eq4}^2}{\gamma_4}}}\right)$$
$$+ Q\left(\frac{\sqrt{2}\left(\gamma_1 + \gamma_2 + \gamma_{eq3}\right)}{\sqrt{\gamma_1 + \gamma_2 + \frac{\gamma_{eq3}^2}{\gamma_3}}}\right) + Q\left(\sqrt{2\left(\gamma_1 + \gamma_2\right)}\right).$$

$$(4.35)$$

Finally, by obtaining and weighting the conditional error probabilities for all error vector patterns we get

$$P(\hat{\hat{u}}_1 \neq u_1) \simeq (1 - p_{e4})Q\left(\frac{\sqrt{2}\left(\gamma_1 + \gamma_{eq4}\right)}{\sqrt{\gamma_1 + \frac{\gamma_{eq4}^2}{\gamma_4}}}\right)$$
$$+ p_{e4}Q\left(\frac{\sqrt{2}\left(\gamma_1 - \gamma_{eq4}\right)}{\sqrt{\gamma_1 + \frac{\gamma_{eq4}^2}{\gamma_4}}}\right) + Q\left(\sqrt{2\left(\gamma_1 + \gamma_2\right)}\right), \quad (4.36)$$

where the terms which decrease with $\bar{\gamma}^3$ are neglected. If we use the two-dimensional sampling property results of Section 4.1.1 in finding the expectation of the instantaneous BER (4.36), we approximate the average BER expression for u_1 with

$$E_{\gamma_1,\gamma_2,\gamma_4,p_{e4}}\left\{P(\hat{\hat{u}}_1 \neq u_1)\right\} \approx \frac{1}{16\bar{\gamma}^2}\exp\left(-\frac{1.3049}{\bar{\gamma}}\right) + \frac{3}{8\bar{\gamma}^2}\exp\left(-\frac{1.6394}{\bar{\gamma}}\right)$$
$$+ \frac{4}{16\bar{\gamma}^2}\exp\left(-\frac{3.1301}{\bar{\gamma}}\right). \tag{4.37}$$

Following the same procedure one can obtain the end-to-end BER expressions for u_2 and u_3 as well. Agreement of these derived expressions with the simulation results is shown in Section 4.3.

4.3 Sample Network-I: Analytical Results Comparison

We present the performance figures in this section in order to validate the analysis for the network coded cooperative communication system done in Section 2.2. We give the results for the network coded system introduced in Section 2.2.1 with Fig. 2.3. Initially, we observe the comparison of BER curves for three network decoders based on simulations in Fig. 4.6: the optimal decoder of (2.14), the suboptimal equivalent channel individual decoder of (4.26), and the suboptimal equivalent channel joint decoder of (4.27). Based on this observation, we state that both the equivalent channel assumption and the joint detection simplification have negligible effect on the BER performance of network decoding operation. Thus a valid analysis for the simplest decoder of (4.27) serves as a good performance metric for the optimal decoder of (2.14) as well.

In Fig. 4.7, we present the agreement between the BER curves of the simulations for the joint equivalent channel network decoder of (4.27) and the BER expressions we derive in Section 4.2.2. The simulated performance curves for all data bits are in good agreement with the analysis results for a wide range of SNR values. As a result, the analysis that is using the generalized forms of the sampling property for the Q-function perfectly fits the simulation results for this network coded system of interest.
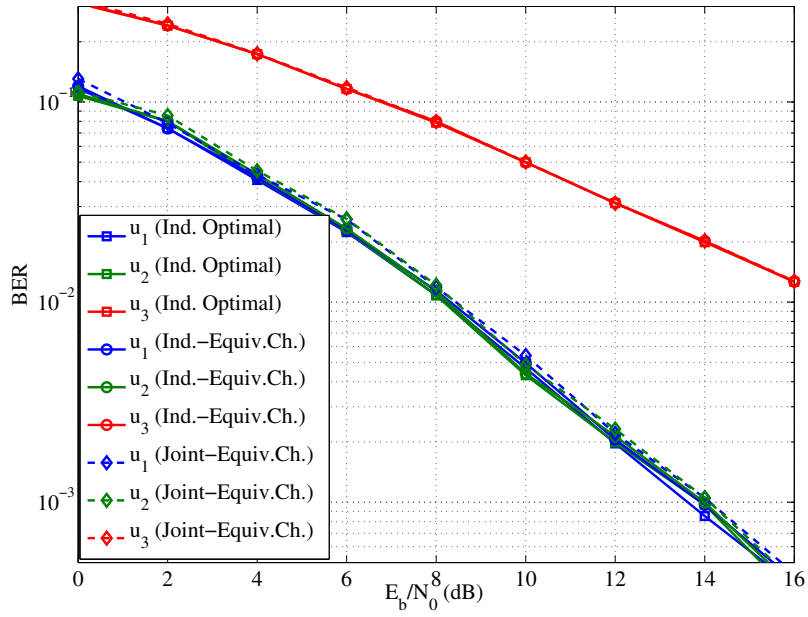
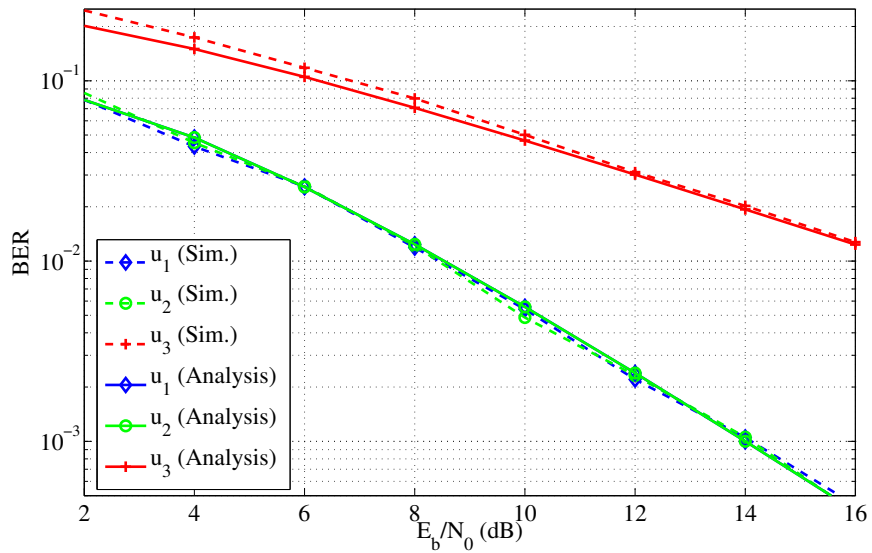Figure 4.6: Performance of the optimal and the equivalent channel decoders

Figure 4.7: Simulation and analysis results for equivalent channel joint decoder

70

4.4 Discussion

This section comprises the second part of this work and deals with derivation of the closed form approximate end-to-end expected BER expressions for both the canonical and NC cooperative communication system models. The generalization of the sampling property of the Q-function to more than one arguments that encompasses the instantaneous BER expressions for these systems is a crucial part of derivation. Other two important techniques worth mentioning are the equivalent channel approach and the C-MRC method that we adopt to both the decoders and the analysis of the NC systems. We also present a rigorous investigation of the sampling property and an SNR-based characterization for selection of the sampling functions for an example integral approximation problem. Finally we combine all these proposed analysis techniques in order to reach the closed form average BER expressions for Sample Network-I and demonstrate the accuracy of these expressions in comparison with the simulation results. We should note that the analysis steps covered in this section may be generalized for the analysis of a larger network with a hierarchical structure, for which the small sub-networks can be seen as the building blocks we describe herein. In this way, one may model and analyze structures with more than one intermediate node being involved in the NC process before a data packet reaches its destination. Accordingly, each new intermediate node of a level may be seen as the destination for the previous level and analysis of the end-to-end average BER values can be done level-by-level.

We expect that the analysis techniques utilized in this section, particularly the generalized sampling property for the Q-function is applicable for the performance analysis of many other systems than cooperative communications with little modifications. The required improvements on the technique include generalization to the expectation integrals involving correlated random variables and arbitrary fading distributions.

CHAPTER 5

CONCLUSION AND DISCUSSION

In this work, we formulate a network coded (NC) communication system problem for cooperative unicast transmissions carried out using orthogonal time slots in a wireless network. The idea behind this formulation is to propose and analyze a miniaturized network structure with a few nodes that may be useful for the design and performance evaluation of a larger network composed of many of these building blocks. For defining the operations realized within such a building block, a generator matrix $\mathbf{G}$ and a scheduling vector $\mathbf{v}$ are used and this pair represents the linear combinations performed at the intermediate nodes. We present a MAP-based decoding rule utilizing $\mathbf{G}$, $\mathbf{v}$, and the error probabilities at the intermediate nodes. A method for obtaining the performance determining parameter as the diversity order for individual source nodes is proposed for any given $\mathbf{G}$ over the corresponding separation vector. Through simulations we show that our decoding rule, using reliability information for the network coded symbols, avoids the possible diversity order losses that may stem from the error propagation effect. We present design examples for network codes via greedy block codes, which may also provide unequal diversity orders to different nodes with proper puncturing. Over given design examples, we obtain rate-diversity trade-off curves and a rate advantage realized by using NC with respect to the no NC case. Moreover, we introduce the sum-product (SP) algorithm based iterative network decoder which has linear complexity order and performs quite close to the optimal rule. Furthermore, the selective NC scheme that combines only the reliably detected data at cooperating nodes is shown to yield additional coding gains.

As another important contribution, we derive some useful average BER expressions

in closed form for both the basic relayed and the proposed network coded communication scenarios under Rayleigh block fading. In order to obtain these closed form expressions, we generalize the sampling property of the Q-function that is frequently observed in instantaneous BER functions of these systems. This generalization includes an insightful analysis of the applicability of the sampling property in addition to the extension of it to integrands of more than one variables. We also propose a network decoder which operates under equivalent channel assumption based on C-MRC method. By combining two independent paths from a source and an intermediate node to the destination under a single channel, this assumption enables both reduction in the complexity of the analysis and the decoding with a negligible loss in performance. We substantiate the validity of these generalizations on sampling property for integrals and the use of equivalent channel assumption together with C-MRC in network coded systems through extensive simulations.

The gains obtained by using NC particularly together with the selective coding idea are notable when the source and the intermediate nodes in the network have the chance of transmitting their data through independently fading links. In addition, under slower fading channels whose coherence durations are on the order of several packets, the gains in BER performance with respect to the conventional repetition methods similar to ARQ is shown to be even larger. On the other hand, when the links between the destination node and the intermediate nodes are correlated, one should expect little improvement due to NC.

Another important point is that the distributed NC described here is based on very short blocklength codes and no channel coding is assumed. In a realistic scenario, one can support these network codes by good channel codes. The joint decoding of the channel and the network codes on a single graph structure by using the SP algorithm is also possible with very low complexity. Moreover, one may also add the effect of channel estimation errors into this graph and investigate possible interference cancellation techniques for even more realistic scenarios. However, under a nonorthogonal transmission model with interfering signals, the results we reach here may change on the favour of a non-NC technique by taking the additional complexity and decoding delay we impose on the intermediate and the destination nodes. As an example on the delay argument, for a round of communication consisting of $n =$

10 intermediate node transmissions, a destination node must wait completion of all packet transmissions to start decoding a desired packet, which may be a problem for delay intolerant applications.

The system model we propose for NC in this work also relies on the assumption that every node in the network has information in its buffer to transmit whenever it is scheduled to use the channel. However, in a scenario with some nodes having bursty traffic for small durations and have no data for the remaining time, it may be better to keep such nodes silent particularly if their assistance to other nodes is negligible and energy sources are scarce. From this point of view, in order to apply NC, one has to consider adaptively arranging the scheduling vectors and the generator matrices in each round of communication based on the node queue lengths and energy constraints. Moreover, in the case that average channel strengths are not homogeneous throughout the network, the fixed generator matrix and scheduling vector assignment in our model should be changed as well. In order to support networks with many nodes (on the order of hundreds), one may prefer long blocklength codes like LDPC codes since the regular block codes discussed in this work (like greedy codes) are NP-hard to generate for increasing number of users. One may further generalize the model here by not only network coding within a round of communication but also coding packets originating from different rounds, which is known in the literature as inter-session network coding. Inter-session NC would in fact be a necessity for a real system in which a packet that could not be delivered in a round has to be injected in to the network once more in the consecutive round.

Identifying gains of NC for purely random **G** matrices in large networks, studying the effects of imperfect information on channel gains and relay error probabilities may be addressed in future work. It would be also interesting to operate the suggested wireless NC methods under asymmetrical channel gains, which can be more realistic for ad hoc networks. Finally, the adaptation of these methods to various types of fading channels and to the scenarios including correlated channels seem to be other open problems.

The idea of approximating some part of the integrand with a Dirac-delta for a hard-to-evaluate expectation integral seems to be a solution more general than the one for

obtaining the performance figures of the cooperative NC systems defined herein. With this reasoning and the high accuracy of the sampling property for NC system analysis in mind, we expect that the methods presented in this work are easy to adapt to many other communications problems. However, this adaptation requires investigation on application of the sampling property to integrands involving joint pdfs with correlated random variables, providing analytical ways of obtaining the impulse weights of the sampling functions, improving the low-SNR accuracy through truncated series approximations on the sampled functions, and classifying a given function according to its suitability of being a sampling function through rigorous analysis. Therefore, one has to be careful in utilizing the sampling property to approximate a given integral and check the applicability through the constraints we mentioned in this work.

REFERENCES

[1] R. Ahlswede, N. Cain, S. Li, and R. Yeung. Network information flow. *IEEE Trans. Inf. Theory*, 46:1204–1216, Jul. 2000.

[2] E. Aktas, J. Evans, and S. Hanly. Distributed decoding in a cellular multiple-access channel. *IEEE Trans. on Wireless Commun.*, 7(1):241 –250, Jan. 2008.

[3] T. Aktas, A. Yilmaz, and E. Aktas. Practical wireless network coding and decoding methods for multiple unicast transmissions. In *IEEE Wireless Commun. and Networking Conference (WCNC)*, pages 6–11, 2012.

[4] T. Aktas, A. Yilmaz, and E. Aktas. Generalizing the sampling property of the q-function for error rate analysis of cooperative communication in fading channels. In *Information Theory Proceedings (ISIT), 2013 IEEE International Symposium on*, pages 46–50, 2013.

[5] T. Aktas, A. Yilmaz, and E. Aktas. Performance analysis of network coded systems under quasi-static rayleigh fading channels. *Submitted to IEEE Trans. Commun., http://arxiv.org/abs/1312.1593*, Dec 2013.

[6] T. Aktas, A. Yilmaz, and E. Aktas. Practical methods for wireless network coding with multiple unicast transmissions. *IEEE Trans. Commun.*, 61(3):1123–1133, 2013.

[7] I. E. Bocharova, F. Hug, R. Johannesson, and B. D. Kudryashov. A greedy search for improved qc ldpc codes with good girth profile and degree distribution. In *2012 IEEE International Symposium on Information Theory*, pages 3083 –3087, Jul. 2012.

[8] J. Boutros, A. Guillen i Fabregas, E. Biglieri, and G. Zemor. Design and analysis of low-density parity-check codes for block-fading channels. In *Information Theory and Applications Workshop, 2007*, pages 54 –62, Feb. 2007.

[9] R. A. Brualdi and V. Pless. Greedy codes. *Journal of Combinatorial Theory Series A*, 64(1):10–30, Sep. 1993.

[10] G. Caire, G. Taricco, and E. Biglieri. Bit-interleaved coded modulation. *IEEE Trans. Inf. Theory*, 44(3):927–946, 1998.

[11] D. Chen and J. Laneman. Modulation and demodulation for cooperative diversity in wireless systems. *IEEE Trans. Wireless Commun.*, 5(7):1785 –1794, Jul. 2006.

[12] G. Colavolpe and G. Germi. On the application of factor graphs and the sum-product algorithm to isi channels. *IEEE Trans. Commun.*, 53(5):818 – 825, May. 2005.

[13] M. Di Renzo, M. Iezzi, and F. Graziosi. Beyond routing via network coding: An overview of fundamental information-theoretic results. In *in Proc. IEEE Int. Symposium on PIMRC*, pages 2745 –2750, Sep. 2010.

[14] M. Di Renzo, M. Iezzi, and F. Graziosi. Diversity and coding gain of multi-source multi-relay cooperative wireless networks with binary network coding. *CoRR*, abs/1109.4599, 2011.

[15] R. Gallager. Low-density parity-check codes. *IRE Trans. Inf. Theory*, 8(1):21–28, 1962.

[16] Y. Gao, J. Ge, and C. Han. Performance analysis of differential modulation and relay selection with detect-and-forward cooperative relaying. *IEEE Commun. Lett.*, 15(3):323–325, 2011.

[17] A. Goldsmith. *Wireless Communications*. Cambridge Univ. Press, 2005.

[18] P. Herhold, E. Zimmermann, and G. Fettweis. A simple cooperative extension to wireless relaying. In *Communications, 2004 International Zurich Seminar on*, pages 36 – 39, 2004.

[19] T. Ho, M. Medard, R. Koetter, D. Karger, M. Effros, J. Shi, and B. Leong. A random linear network coding approach to multicast. *IEEE Trans. Inf. Theory*, 52:4413 –4430, Oct. 2006.

[20] M. Iezzi, M. Di Renzo, and F. Graziosi. Closed-form error probability of network-coded cooperative wireless networks with channel-aware detectors. In *IEEE GLOBECOM 2011)*, pages 1 –6, Dec. 2011.

[21] M. Iezzi, M. Di Renzo, and F. Graziosi. Network code design from unequal error protection coding: Channel-aware receiver design and diversity analysis. In *2011 IEEE International Conference on Commun.*, pages 1 –6, June 2011.

[22] M. Iezzi, M. D. Renzo, and F. Graziosi. *Flexible Network Codes Design for Cooperative Diversity, Adv. Trends in Wireless Commun.* InTech, 2011.

[23] A. Jalil and A. Ghrayeb. Improved diversity-multiplexing tradeoff for underwater acoustic channels based on distributed channel coding. In *Personal Indoor and Mobile Radio Communications (PIMRC), 2013 IEEE 24th International Symposium on*, pages 1249–1254, 2013.

[24] W. M. Jang. Quantifying performance in fading channels using the sampling property of a delta function. *IEEE Commun. Lett.*, 15(3):266 –268, Mar. 2011.

[25] W. M. Jang. Quantifying performance of cooperative diversity using the sampling property of a delta function. *IEEE Trans. Wireless Commun.*, 10(7):2034 –2039, Jul. 2011.

[26] W. M. Jang. Dynamic integration using sampling in fading channels. *IEEE Trans. Commun.*, 60(10):2768 –2775, Oct. 2012.

[27] B. Jenkins. Tables of lexicodes. http://burtleburtle.net/bob/math/ lexicode.html. [Online; accessed 07-May-20012].

[28] S. Katti, H. Rahul, W. Hu, D. Katabi, M. Medard, and J. Crowcroft. Xors in the air: Practical wireless network coding. *IEEE/ACM Trans. Netw.*, 16(3):497 –510, Jun. 2008.

[29] D. Kim, H.-M. Kim, and G.-H. Im. Improved network-coded cooperative transmission with low-complexity adaptation to wireless channels. *IEEE Trans. Commun.*, 59(10):2916–2927, 2011.

[30] J. Laneman, D. Tse, and G. Wornell. Cooperative diversity in wireless networks: Efficient protocols and outage behavior. *IEEE Trans. Inf. Theory*, 50(12):3062 – 3080, Dec. 2004.

[31] J. Li, J. Yuan, R. Malancy, M. Xiao, and W. Chen. Full-diversity binary framewise network coding for multiple-source multiple-relay networks over slow-fading channels. *IEEE Trans. Veh. Technol.*, 61(3):1346 –1360, Mar. 2012.

[32] L. Lu, M. Xiao, M. Skoglund, L. Rasmussen, G. Wu, and S. Li. Efficient network coding for wireless broadcasting. In *Wireless Communications and Networking Conference (WCNC), 2010 IEEE*, pages 1 –6, Apr. 2010.

[33] D. J. MacKay. Good error-correcting codes based on very sparse matrices. *IEEE Trans. Inf. Theory*, 45(2):399–431, 1999.

[34] L. Monroe and V. Pless. Greedy generation of non-binary codes. In *1995 IEEE International Symposium on Information Theory (ISIT)*, page 235, Sep. 1995.

[35] T. Moon. On general linear block code decoding using the sum-product iterative decoder. *IEEE Commun. Lett.*, 8(6):383 – 385, Jun. 2004.

[36] A. Nasri, R. Schober, and M. Uysal. Performance and optimization of network-coded cooperative diversity systems. *IEEE Trans. Commun.*, 61(3):1111–1122, 2013.

[37] H. V. Nguyen, S. X. Ng, and L. Hanzo. Performance bounds of network coding aided cooperative multiuser systems. *IEEE Signal Process. Lett.*, 18(7):435 – 438, Jul. 2011.

[38] F. Onat, A. Adinoyi, Y. Fan, H. Yanikomeroglu, J. Thompson, and I. Marsland. Threshold selection for snr-based selective digital relaying in cooperative wireless networks. *IEEE Trans. Wireless Commun.*, 57:4226–4237, Dec. 2008.

[39] J. G. Proakis. *Digital Communications*. McGraw-Hill, 2001.

[40] T. Richardson and R. Urbanke. The capacity of low-density parity-check codes under message-passing decoding. *IEEE Trans. Inf. Theory*, 47(2):599–618, 2001.

[41] A. Sendonaris, E. Erkip, and B. Aazhang. User cooperation diversity. part I and II: Implementation aspects and performance analysis. *IEEE Trans. Commun.*, 51(11):1939 – 1948, Nov. 2003.

[42] R. Tanner. A recursive approach to low complexity codes. *Information Theory, IEEE Transactions on*, 27(5):533–547, 1981.

[43] W. van Gils. Two topics on linear unequal error protection codes: Bounds on their length and cyclic code classes. *IEEE Trans. Inf. Theory*, 29(6):866 – 876, Nov. 1983.

[44] C. Wang, M. Xiao, and M. Skoglund. Diversity-multiplexing tradeoff analysis of coded multi-user relay networks. *IEEE Trans. Commun.*, 59(7):1995 –2005, Jul. 2011.

[45] L. Wang, W. Liu, and S. Wu. Analysis of diversity-multiplexing tradeoff in a cooperative network coding system. *IEEE Trans. Commun.*, 59(9):2373–2376, Sep. 2011.

[46] T. Wang, A. Cano, G. Giannakis, and J. Laneman. High-performance cooperative demodulation with decode-and-forward relays. *IEEE Trans. Commun.*, 55:1427–1438, Jul. 2007.

[47] T. Wang, G. Giannakis, and R. Wang. Smart regenerative relays for link-adaptive cooperative communications. *IEEE Trans. Commun.*, 56:1950–1960, Mar. 2008.

[48] S. B. Wicker. *Error control systems for digital communication and storage.* Prentice-Hall, Inc., Upper Saddle River, NJ, USA, 1995.

[49] M. Xiao and T. Aulin. Energy-efficient network coding for the noisy channel network. In *2006 IEEE International Symposium on Information Theory (ISIT)*, pages 778 –782, Jul. 2006.

[50] M. Xiao and T. Aulin. On the bit error probability of noisy channel networks with intermediate node encoding. *IEEE Trans. Inf. Theory*, 54(11):5188 –5198, Nov. 2008.

[51] M. Xiao and T. Aulin. Optimal decoding and performance analysis of a noisy channel network with network coding. *IEEE Trans. Commun.*, 57:1402–1412, 2009.

[52] M. Xiao and M. Skoglund. Multiple-user cooperative communications based on linear network coding. *IEEE Trans. Commun.*, 58(12):3345 –3351, Dec. 2010.

[53] S. Yang and R. Koetter. Network coding over a noisy relay: a belief propagation approach. *in Proc. IEEE International Symposium on Information Theory, Jun. 2007*.

[54] J. Yuan, Y. Li, and L. Chu. Differential modulation and relay selection with detect-and-forward cooperative relaying. *IEEE Trans. Veh. Technol.*, 59(1):261–268, 2010.

CURRICULUM VITAE

PERSONAL INFORMATION

Surname, Name: Aktaş, Tuğcan
Nationality: Turkish (TC)
Date and Place of Birth: 23.01.1983, Ankara
Marital Status: Single
Phone: 0312 286 20 21
Fax: 0312 210 2304

EDUCATION

Degree	Institution	Year of Graduation
M.S.	Middle East Technical University	2007
B.S.	Middle East Technical University	2005
High School	Atatürk Anadolu High School	2001

PROFESSIONAL EXPERIENCE

Year	Place	Enrollment
12/2009 - 1/2014	Middle East Technical University	Research Assistant

PUBLICATIONS

1- Aktas, T.; Yilmaz, A.O.; Aktas, E., "Practical Methods for Wireless Network Coding With Multiple Unicast Transmissions," Communications, IEEE Transactions on ,

vol.61, no.3, pp.1123,1133, March 2013

2- Aktas, T.; Yilmaz, A. O.; Aktas, E. "Performance Analysis of Network Coded Systems Under Quasi-static Rayleigh Fading Channels," arXiv preprint arXiv:1312.1593. Submitted to IEEE Trans. Commun. (Dec 2013)

International Conference Publications

3- Aktas, T.; Yilmaz, A.O.; Aktas, E., "Generalizing the sampling property of the Q-function for Error Rate analysis of cooperative communication in fading channels," 2013 IEEE International Symposium on Information Theory Proceedings (ISIT), pp.46,50, 7-12 July 2013

4- Aktas, T.; Yilmaz, A.O.; Aktas, E., "Practical wireless network coding and decoding methods for multiple unicast transmissions," 2012 IEEE Wireless Communications and Networking Conference (WCNC), pp.6,11, 1-4 April 2012

5- Sen, P.; Aktas, T.; Yilmaz, A.O., "A Low-Complexity Graph-Based LMMSE Receiver Designed for Colored Noise Induced by FTN-Signaling," 2014 IEEE Wireless Communications and Networking Conference (WCNC), 6-9 April 2014, Accepted

6- Guvensen, G.M.; Aktas, T.; Yilmaz, A.O., "Probability of full-diversity for simple coded and rotated multidimensional constellation systems," Personal, Indoor and Mobile Radio Communications, 2009 IEEE 20th International Symposium on , vol., no., pp.885,889, 13-16 Sept. 2009